UNIVERSITY OF THE WEST of SCOTLAND

UWS

School of Computing,
Engineering & Physical Sciences

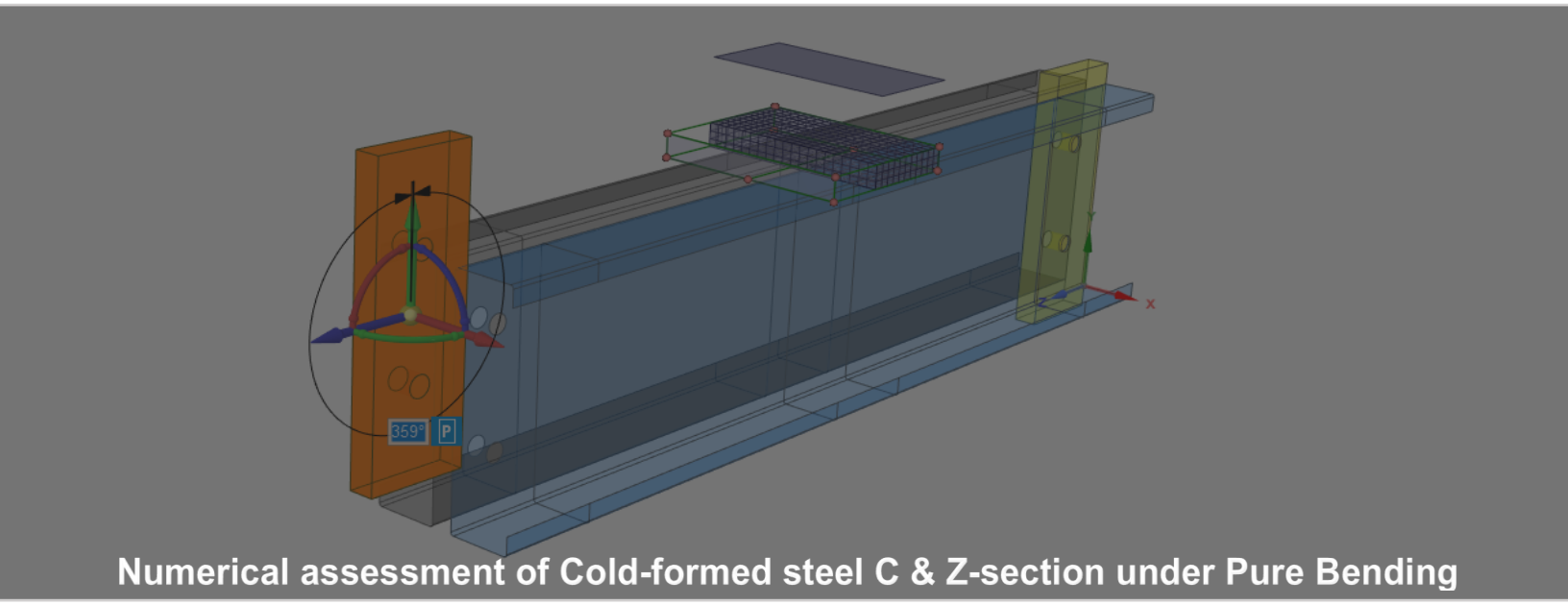


# Mechanical Engineering

Thapa, Hemant

B00380494

Supervisor: Dr Asraf Uzzaman

School of Engineering

Paisley College of Technology

The University of the West of Scotland

2020

## Abstract

Increased use of web openings in cold-formed steel load bearings, such as wall studs or floor joints, is made to promote services in buildings. Web crippling will occur at points of concentrated loads in such members, which will be affected by the openings' size and location. The material thickness and strength of the channel segment are improved due to the enhancement of cold-formed techniques, but research is limited on the cold-formed steel members with web openings. This paper details the finite element code of conduct for a variety of load cases to model cold-formed steel-lipped channel and Zed sections subject to bending conditions. The code was constructed parametrically, meaning that every single value needed to build the models are given, a parameter that could be easily changed to create a powerful analysis tool for this type of steel segment.

# Acknowledgments

First of all, I would like to express my sincere gratitude to my supervisor, Dr. Asraf Uzzaman, and the people who have contributed, in different ways to the completion of my honors-level study at the school of engineering at the University of the West of Scotland, for providing me guidance, encouragement, support throughout and invaluable advice throughout my studies.

I wish to thanks my module Coordinator and lecturer Dr. Bassam Rakhshani for providing me with an opportunity to undertake this project on behalf of the university.

I am sincerely thanks my lecturer Dr. Tony Leslie and Dr. Tony murmur for their valuable contribution in teaching me design-related problems, their continuous support and guidance throughout the composite structure and design analysis has contributed plus played a vital role for gathering information regarding this project.

I gratefully thank Dr. Esther smith and Dr. Obeid Obeid from my University, who help me and provided me great material for understanding analysis and simulation software, using PTC Creo and ANSYS, their teaching videos have always educated me, and material has also help me to self-study and develop my interest toward Autocad.

I wish to record my grateful appreciation to all my lecture and instructor from previous Academy and College, B.P Marine Academy, and City of Glasgow college nautical campus who educated me and provided me continuous support throughout, my successful completion of Marine engineering studies and encouraged me to pursue my entire future study in the UK.

Special, thanks to my dearest parents for all the loved encouragement throughout my life, my fulfillment of educating myself would have not been possible without them.

# Deceleration

I, the undersigned, hereby declare that this research thesis is my original work and all the sources have been accurately reported and acknowledged, various sources are involved for the successful completion of this thesis, which includes the Previously published book, various university library material, internet, current affairs and except specific references have been made to the relevant work of other. No portfolio has been invested during this research and this document has not been previously submitted to any University to obtain academic qualifications.

A thesis submitted in completed single document fulfillment of the requirements of MEng in Mechanical Engineering

Word count of the thesis: 10,923 words (within 10000 + 10%)

Table count of the thesis: 6 tables

Figure count of the thesis: 74 figures

External Contact

Email: hemantthapa63@gmail.com

LinkedIn: https://www.linkedin.com/in/thapahemant/

Research gate: https://www.researchgate.net/profile/Hemant_Thapa3

ORCID Id: https://orcid.org/0000-0002-7641-8505

Hemant Thapa

B00380494

05.05.2021

# Contents

# List of figures

## List of tables

# Nomenclature

| | |
|---|---|
| CFS | Cold-formed steel |
| LGS | Light Gauge steel |
| FEA | Finite Element Analysis |
| FE | Finite Element |
| APDL | ANSYS parametric design language |
| BS | British Standard |
| Z- Section | Zed section |
| C- Section | Channel section |
| 2D | Two dimensional |
| 3D | Three dimensional |
| HSS | Hollow structural section |
| RHS | Rectangular hollow sections |
| SHS | Square hollow sections |
| CHS | Circular hollow sections |
| LFS | Light steel framing |
| W | Width |
| L | Length |
| T | Thickness |
| IOF | Interior-one-flange |
| EOF | End –one-flange |
| ETF | End to flange |
| ITF | Interior two flange |
| UTS | Ultimate tensile strength |
| A | Alpha |
| B | Beta |

# Chapter 1 (Introduction)

## 1.1 Introduction

Cold form steel (CFS) maintains a dominant presence in the various industry in the construction of building, marine industry (merchant navy), aircraft industry, oil, and gas industry. The result of continuous development in material properties through a transition from traditional lab-based experimental techniques performed in the workshop, to virtual simulation techniques performed in a computer has shaped our world and played a vital role in the study regarding behavior in the structure. which prompt an increase in the production of the CFS, construction technique, and innovation design. channel and zed section play vital roles in the structural application of the design, principal to their favorable structural properties present various advantages into the production of steel and prefabrication. Research data from the last few decades have witnessed their widespread application in various landmarks and complex structures with successful designs around the world.

Figure 1: Cold-formed Steel Roof Purlins

Figure 2: Cold-Formed Steel Studs Framing


(a)

(b)

Figure 3: (a) & (b) - The Hong Kong and Shanghai Bank Corporation (HSBC) Headquarters Building

Cold-formed steel can be formed into desirable shapes at room temperature or ambient temperature. They are general manufactured from thin steel sheets. The manufacturing process is done by pressing and rolling at room temperature is light gauge steel or may also be referred to as CFS. The term “cold” is used because this type of steel product is manufactured at room temperature. The Term “C” and “Z” refer to their structure profile bar which comes under the open section. The plan C and Z sections are one of the most common cold form steel purlin used in a daily roof system. The thin wall characteristic of steel is highly demanded in the market for lightweight structure and greater strength quality. Its lapping capacity provides continuity in the support regions, double thickness material contributes to better performance and more economical designs. The production of cold-formed steel members with high strength has led to an increase in the use of steel purlin in both commercial and industrial structures. Systematic research work has been undertaken for the past 40 years to develop manufacturing technology. Increasing the strength of the material, and protecting against corrosion, has led cold form steel into wider usage in building industries.

CFS is one of the fastest-growing branches of the structural steel market. Steel is the most versatile material to recycle, the world steel maker recycles about 500million tons of steel every year, it takes less than 60% of energy to recycle steel from scrap rather than using iron ore to produce steel. In the United Kingdom, CFS was available for more than 150 years before the first guideline produces but didn’t utilized until 1946, the United State of Iron and steel research institute introduced the first guideline for use of cold-formed steel. The guideline contains about permissible loads for cold-formed steel section can support. These help engineers to make more efficient decisions and types of a section have been introducing for a significant role. Every year researcher conducts their research on CFS over the globe and makes a continuous update on behavior since 1946, as well as an improvement into design IT tools, have provided accurate result and complex design are getting possibly safer with a calculated risk factor. There is no surprise that the demand for CFS steel is rising every day.


(a) (b)

Figure: 4 (a) & (b): cold-formed steel purlins in use for roof systems

## 1.2 The motivation of the research

Increasing in use of cold-formed steel in modern society, there is an essential need for a more efficient design methodology to develop CFS structures. The full stress-strain response of cold-formed steel and hot-rolled steel is defined by precise models. which allows the structure to be simulated and designed according to the specific material properties.

1. To design and manufacture a FE model with a finite element package using ANSYS workbench.
2. To develop the 2D and 3D models of the C section and Z section.
3. To validate simulation results with the experiment, it reduces the costing and the time required for experimental investigation performed into a workshop.
4. To study and investigate the effect of the load applied on the material causes collapse loads.
5. The Comparison will be conducted between experimental literature data and numerical results with the design strength predicted by the current design code.

## 1.3 Methodology

To achieve the desirable aforementioned aim and objective through the project, in-depth understanding of the structural performance of the CFS into commercial and industrial usage, an extensive literature review is conducted to understand the contribution of research paid by various researcher and journalist, into continuous progression for the development of CFS due to previous publish research paper has been examined, regarding the relevant topic of CFS and also identifying the existing gap of knowledge. A series of laboratory tests have been conducted to obtain the data of C section and Z section beam behavior. The test result and outcomes from existing previous published papers are studies and also used for references. The test result is used for validation of numerical simulation. FEA techniques are employed to mathematically model and numerically solve complex structural problems. The ANSYS-WORKBENCH packages will develop a key component from a building structure using a 2D and 3D analytical model. Based on the evidence of a test and numerical analysis performed during the project, will guide for the development of the FE designing tool.

## 1.4 Structure of the thesis

- Chapter 1 - General introduction
- Chapter 2 - Literature review
- Chapter 3 - Design and Analysis
- Chapter 4 - Development of the finite element c and z model
- Chapter 5 - Model setup
- Chapter 6 - Parametric Study
- Chapter 7 - Conclusion & Further Work

## 1.5 Summary

This chapter addressed the background of the thesis, novelty, the aim and the objectives and methodology approaches to an investigation. Each thesis chapter represents the task undertaken during the research. The details of the research are presented in the following chapters.

# Chapter 2 (Literature review)

## 2.1 Introduction

This chapter provides an overview of previous research into CFS and the design aspect relevant to this thesis, literature is introduced and reviewed in subsequent individual chapters. This chapter consists of both experimental and analytical investigation into cold-formed sections of various cross-sectional shapes from the structure profile bar. The work follows from previous relevant work which is undertaken through FE model simulation and various source of approaches has taken to get an efficient result.

This chapter review, the stress-strain behavior of the material, structural profile, manufacturing process, advantages and disadvantages of CFS, etc. summary of the development of CFS structural design guidance covering the United Kingdom, United States, European countries, Australia and New Zealand. this is followed by and review of the design approaches for the prediction of collapse load. All collective data and analysis will perform through design standards, and a more essential method is proposed in the literature.

### 2.2.1 Historical Review

The use of the CFS structure is just about as old as the hot-rolled steel variety. Both started their development around the 1850s in the United States and the United Kingdom. In between the 1920s and 1930s, there was also limited acceptance of cold-formed steel as a construction material. Since there was no appropriate design specification and limited material usage knowledge in building codes. The Virginia Baptist Hospital is one of the earliest documented use of CFS as a construction material, the building is constructed around 1925 in Lynchburg, Virginia, U.S. The floor system was framed with double back-to-back CFS-lipped channels.

Earlier century, with the idea of the invention of the aircraft, an overriding need to form the lightest structure as possible. This was successful achieved by using a thin metal sheet to which stiffeners (Stringers) were riveted.


Figure 5: The Virginia Baptist Hospital

Figure 6: Aircraft wing spar rib Diagram

The cold-formed steel section has become very popular in structural applications in the U.K since the 1960s. In the steel market of the United Kingdom, “METSEC” is the one the largest growing specialist for the cold-rolled forming steel company, they provide products for manufacturing industries and construction company. Lipped channel section and Zed section is the most demanded product, both C and Z section will be referring in this research.

### 2.2.2 Article Review from journal worldwide

Previous studies on the web crippling behavior of cold-formed steel members concentrated mostly on plain channel sections with no web openings. Among others, these include work by Karren and Winter [1], Baeher [2], Cornell [3], Hetrakul and Yu [4], Schuster [5] and Wing [6], Santaputra et al. [7], Sivakumaran [8], Bakker [9], Schuster and Parabakaran [10], Setiyono [11], Cain et al. [12], Young and Hancock [13], Rhodes and Nash [14] Gergesand Schuster [15], Shaojie et al. [16], Baehre and Schuster [17], Hofmeyer et al. [18], Kaspers [19], Holesaple and LaBoube [20], Kaitila [21], Ren et al. [22] and Heiyantuduwa [23], Web crippling expressions without the web for CFS members some of these investigations have indicated opportunities. Design codes have regulations without web openings for cold-formed steel sections, such as the British Norm [24], Eurocode 3 [25], and Specification for North America [26].

Recent research on web crippling of cold-formed steel channel parts includes work by Natario et al. [27], Keerthan, which was again considered without a web opening case. Chen et al. [28], Gunalan and Mahendran et al. [29], and Chen et al. [30], Online inquiries into the debilitating actions of representatives of cold-formed steel. There are very few web openings and they are not protected by the British Standard [31].

Eurocode 3 [32], Power suggested only in the North American specification [33]. equations of the reduction factor for the case of a circular hole having a direct horizontal. The gap to the near edge of the bearing plates, but only if the flanges are the interior-one-flange (IOF) and end-one-flange (IOF) are attached to the bearing plates. The loading conditions of the flange (EOF). Siva Kumaran and Zielonka [34], Lagan [35], Chung [36], Yu and Davis [37], Zhou and Young [38], LaBoube et al [39], and Assraf Uzzaman et al. [40] Experimental and numerical investigations have been performed on the internet debilitating strength of web holes with cold-formed steel members under end-two-flange (ETF) and interior two-flange (ITF) conditions for loading.

## 2.3 Structure profile bar

### 2.3.1 Open sections & Close section

The reliability of the cold-formed steel section varies with the grade, Slenderness ratio, temperature, etc. is a common area of study. The use of a flat 90° angle, 60° angle, lipped 90º angle T-section, back-to-back lipped channel sections is beneficial for the construction of a transmission tower due to its axial load power.

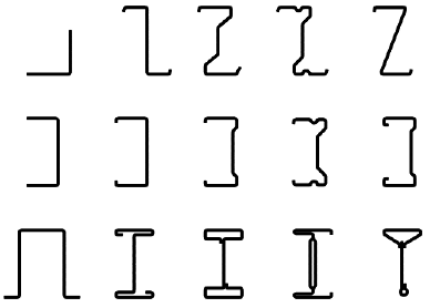

Figure 7: Open section profiles

The steel bar is converted into different shapes C, Z, L, and top hat profile through the manufacturing process. Where, thin-wall sheet through bending, pressing, and rolling acquire such shape profile and dimension of the design depend upon the regulation and factor of safety of the material, their name is given according to their shape structure. Cold-formed steel C and Z section come under open section.

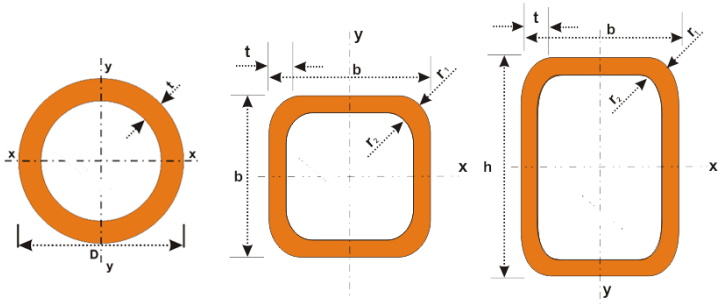


Figure 8: Closed section profiles

Close section structure is a hollow structural section (HSS) is a type of metal profile with a hollow cross-section. Which are categorized into three main types rectangular hollow sections (RHS), square hollow sections (SHS), and circular hollow sections (CHS). Each type of hollow shape section has its specialty, which served its specific purpose.

### 2.3.2 Profiled sheeting

In addition to framing, CFS is also used to provide flooring, roofing, and wall structures. Cold-formed steel panels and decks with various geometry are used in these systems. These elements of cold-formed steel are often used to construct a concrete space. These components are also used to provide ducting for air conditioning, electrical, and heating systems. They are often used to better organize vibration absorption material. To improve the stiffness of these parts, intermediate and edge stiffeners must be used when adding a deeper panel. In general, the depth and thickness of these cold-formed steel panels range from 20 to 200 mm and 0.4 to 1.5 mm respectively.

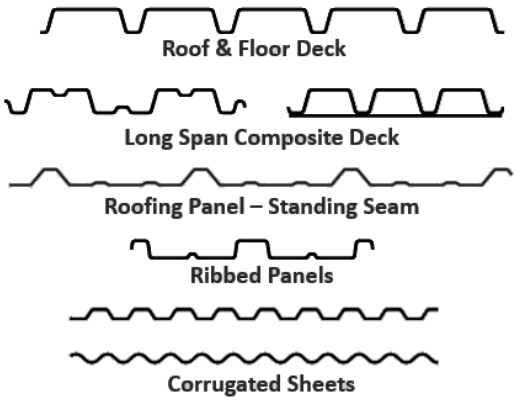


Figure 9: Panel structural profile

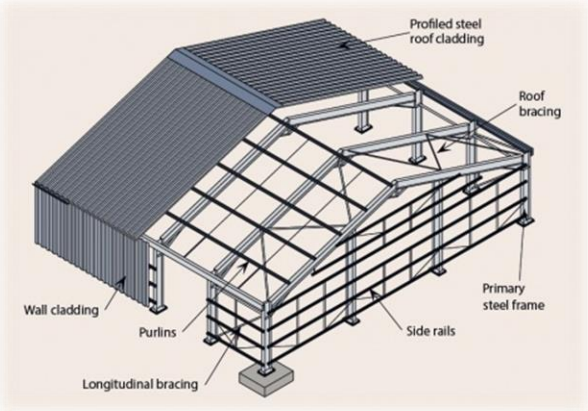


Figure 10: Panel CFS sheet is used in the roofing system

## 2.4 Channel section and Zed Section profile

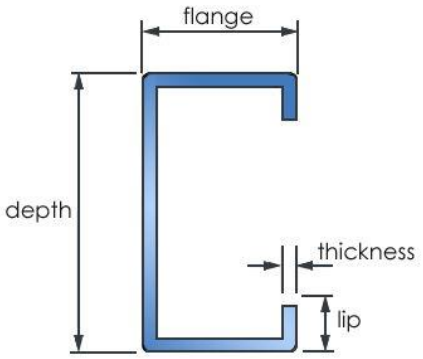


Figure 11: C/Cee/Channel Section

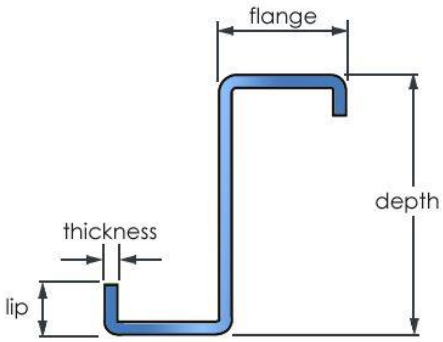


Figure 12: Z/Zed Section

The cold-formed steel channel section and Zed section are categories into two families, lipped and plain channels. The Lipped channel and zed section are utilized for research. Plain channels have additional stiffening lips which figure 11, the flange dimeson is defined by symbol b (figure 13) and web height is define by symbol h (Figure 14).

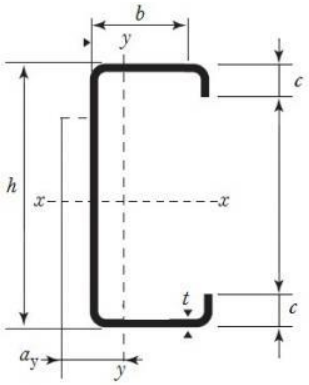


Figure 13: Lipped channel cross-section

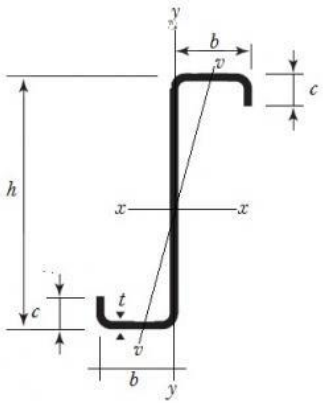


Figure 14: Lipper zed cross-section

Both are used in portal frames, type of structural in construction of building due to their primary advantages high strength to lightweight ratio, provide ease in the manufacturing process, cost-effectiveness due to material reduction and very faster and easier to install with compare to the traditional method of building with the material. It also reduces the construction costing charges, high efficiency of work can be achieved in less amount of time and lightweight property makes it easier to handle the material with construction tools in the construction site.

## 2.5 Fabrication Methodology

There are two types of primary methods used to manufacture CFS sections, rolling forming and brake forming. Coils of a thin sheet which is around 1.5m wide (W) and length (L) wise can be 1000m long. The thickness (T) of CFS varies and depending on the situation and concept of design purpose. The section which is non-structural tends to lies between 0.47mm to 0.79mm of thickness, and the section which tends for structural usage lies between 0.87mm to 3.15mm thick. A list of the variety of an open section can be possible including C and Z sections. The closed section also can be manufactured by running process weld up the seam to seal, the join in the same way as a closed section hot rolled steels are manufactured.

Figure 15: Rolling forming method

In the rolling forming method, the flat strip sheet of steel is forced into series of consecutive pairs of working rolls, which have smooth and high-temperature tolerance surfaces. The metal sheet passes through multi-stage rolls and multi-shape rolls, each stage reduces the dimension of the sheet and produces a new geometrical design. space between each roll decreases and metal sheet express a huge amount of pressure and shape of rolls pair decide the shape of production of the desired section bar shape.

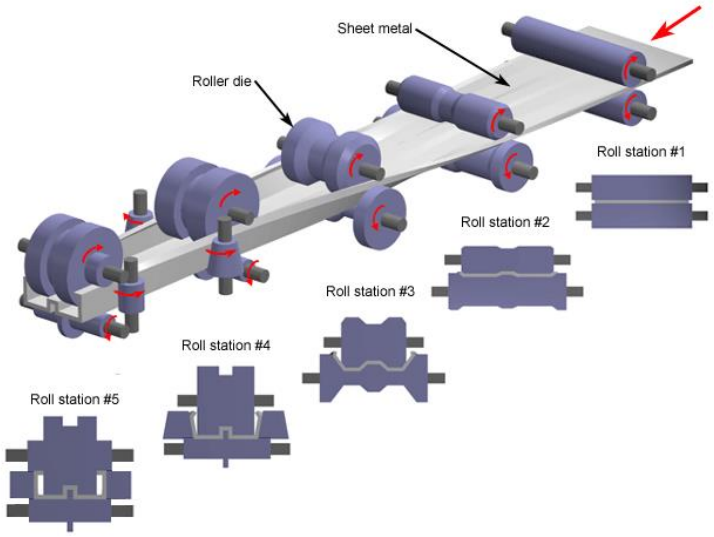


Figure 16: Schematic representation of rolling forming method

In the press braking method of production, the steel sheet is treated as a workpiece and it is placed between dies and punch machine figure 17, the workpiece is bent into desired geometrical shape by placing at dies and exerting force from a punch. To achieve desirable shape bottom tools are fixed in one place and top punching tools move downward direction at speed from 1 mm/s to 15mm/s to force the workpiece to change its shape shown in figure 17, nowadays machines are operated hydraulically but still controlled manually. Bending / Tonnage charts are used for suitable bending and folding, the thickness of the workpiece and configuration of V in the die is needed to be a concern for an appropriate angle between flange and web.

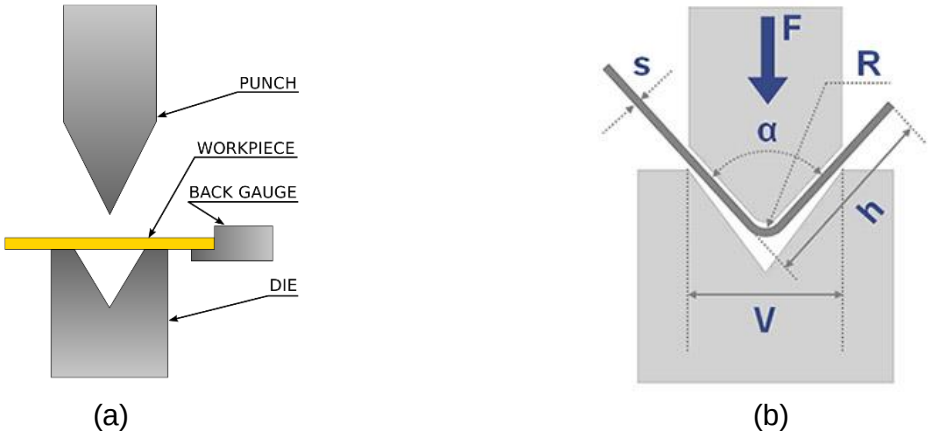


Figure 17: (a)Schematic diagram of press braking & (b) Label diagram representation of press braking

To produce a channel section a flat steel workpiece is selected and needs to undergo multiple bent and it causes large time consuming, it is produced in small scale and especially this roots of production are used for special need of cross-section shape required for any project. The limitation of this product can be seen in the length of the workpiece and it depends on the individual section that is produced. Most of them can produce up to 5m length and some can produce highly up to 8m length.

## 2.6 Material properties

The cold-forming process effect the mechanical advantages of steel structure, it increases yield strength and ultimate strength and also decreases the ductility of the material. The mechanical properties won't cover uniformly across the cross-section of the product due to cold work variation in production. In Cornell University CFS member was investigated by researcher Karren and Winter [1]. Simple unidirectional tensile straining of thin steel sheets to more complex structure types for making the corner and flat sections. The study of investigation has extended the effect of CFS-forming on the applied load-carrying capacity of the material in axially compressed CFS coulombs, which lead to the value of yield strength and UTS at the formed larger as compared to the flat elements which are referred to as hardening effect. Macdonald [41] performed the effect of CFS on the yield stress on thin gauge carbon and stainless steel. A standard hardness test introduces to determine local yield and UTS at the CFS corner. The current code of design permits the CFS structure to make changes in the properties of the material from the CFS manufacturing process. In the United Kingdom, the British standard [42] and Euro code [32] provides rules and regulations for the designs of CFS. Australia/New Zealand standard [43] and North America standard [44] also provide design codes for CFS.

Plasticity is considered for the pure bending analysis. Geometric nonlinearity should be considered for thin-walled structures. the stress-strain curve was adopted to follow the route of elastic-perfectly plastic material; the Von-Mises yield stress formula is used for analysis and the yield stress is **$\sigma_y$=390 MPa**. Elastic perfectly plastic material is determined by **yield strength value of 390 MPa**, **tangent modulus value of 0,** and **Poisson's ratio (v) of 0.3**.

## 2.7 Residual stresses

Residual stresses are stresses that remain in a solid material after the original cause of the stresses has been permanently removed. Residual stress can be desirable or undesirable. In CFS members, it is caused by cold rolled manufacturing process, which plays a vital role in the behavior of the bar profiles under compressive loads. The explanation of adequate computational design modeling of residual stress show trouble. As per result, residual stress needs to exclude for often cases for accurate result or stress-strain behavior of material need to modified to the appropriate effect of residual stresses. In CFS member residual stress is dominated by flexural or through-thickness variation, compare to hot-rolled-steel members residual stress don't vary markedly through its thickness. The raise of variation of residual stress always leads to early yield on the faces of CFS plates. That residual stresses are idealized as a summation of two types which are flexural and membrane figure18.

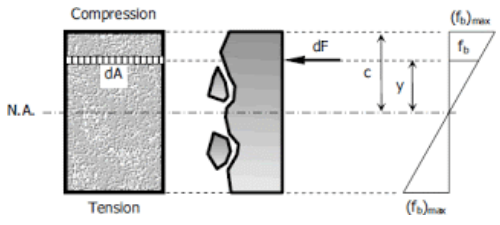


Figure 18: Residual stress distribution

## 2.8 Web crippling Failure

CFS material with thin-walled steel flexural members, floor joists, steel purlins, and decks are often subjected to concentrated applied loads and reaction forces. These concentrated forces show results in various modes of failures which depend upon loading condition in an absence of stiffeners. This mode of failure can be identified as bending failure, shear failure, web crippling failure, and the result can cause the interaction of two or more failures, which is already mentioned above. Web crippling is the center of attention, that may experience through-beam members under concentrated applied load or reaction forces in the beam. In the case of a beam with slender webs, a higher degree can be found in a place where stiffeners have not been applied. Web crippling mode of failure can be identified as a localized failure when web crippling elements just come under the bearing loads (Shown in bottom figure 19).

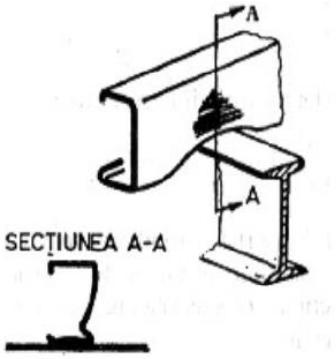


Figure 19: Web crippling at a support point (Rhodes 1994)

Web crippling failure depends upon the various amount of load and also depend upon the types of load conditions, flanges which come under loading condition define whether a load is applied in one flange or both flanges and configuration of load applied and reaction forces applied. If the concentrated load is applied at end of the members, the condition of loading is defined as end loading and similarly, loading condition is concentrated in the middle of the span member then loading condition is defined as interior loading. There are four types of loading condition applied in the web crippling test, EOF end-one-flange loading, IOF Interior one flange loading, end two flange (ETF) loading, and ITF interior two flange loading (shown in bottom figure 20)

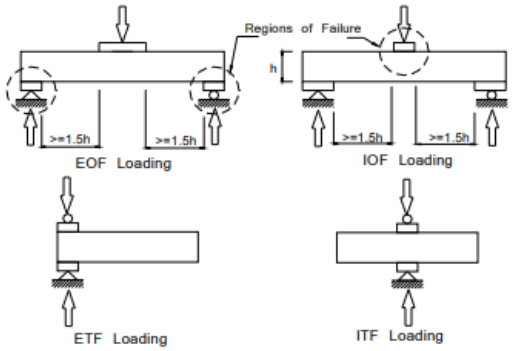


Figure 20: Web crippling loading condition

## 2.9 Summary

The literature review provides information on thin-walled steel, including the manufacturing process, typical section profiles, material properties, buckling failure modes, residual stress in the steel section, and web crippling failure mode. This literature review chapter represents the previous investigation undertaken throughout on the web crippling.

The literature review conducted in web crippling loading conditions in the CFS section indicates, a lack of evidence of research performed on FEA and experimental analysis. The nature of web crippling is very complicated and to achieve an efficient result and more reliable design equation to gain accurate outcome in web crippling failure mode of strength in a different section, more experiment and finite element analysis need to be conducted. A three-point beam bending test will be conduct in Channel and Zed section beam to study the behavior of non-linear material. Reaction force will be generated in beam support members by applying a suitable amount of displacement at $90^{o}$ angle in the middle of the beam.

# Chapter 3 (Design & Analysis)

## 3.1 Introduction

Numerous design parameters influence the efficiency of the bolted web connection and must be taken into consideration during analysis. Such variables are broken down into web and flange dimensions, beam thickness, and applied load. The objective of this chapter is to illustrate for selection of proper design variables, constants, and parameters that should not be neglected during the design phase.

## 3.2 Design variable

For the improvement of safe and quality design of the bolted web connection. different variables are considered carefully, which include web dimensions by span length, section thickness, and applied load. Joints are considered for the durability of the design, lifetime of the structure, cost-efficient, and good corrosion resistance.

### 3.2.1 Section dimension and thickness

The dimension of the web and flange in the C and Z beam has a significant effect on performance during loading conditions. Web and flange deformation, bending strain distribution and flange rotation can cause instability or unreliability into structure due to inappropriate dimensional selection. The safety of the structure not only depends on the material property but also depends on the proper dimensional selection of the beam, for a particular type of loading condition. Minimizing the size of dimension can also reduce the unnecessary requirement of material and save material costing.

While, observing and searching for appropriate data from Bluescope Lysaght company (show in bottom figure 21), steel & pipes for Africa and Tubecon UK (shown in figure 22 & 23). Nominal web size of selection for channel and Zed beam are 75mm to 350mm. Similarly, BMT (Base metal thickness) selection depends on the size of web length or depth which lies between 1mm to 4 mm thickness.

**Standard range of LYSAGHT Zeds and Cees**

| Nominal section size (mm) | BMT (mm) |
|---|---|
| 100 | 1.0, 1.2, 1.5, 1.9 |
| 150 | 1.2, 1.5, 1.9, 2.4 |
| 200 | 1.5, 1.9, 2.4 |
| 250 | 1.9, 2.4 |
| 300 | 2.4, 3.0 |
| 350 | 3.0 |

Figure 21: standard range of Zeds and Cees (Lysaghte)

| | | | | | | | | | | |
|---|---|---|---|---|---|---|---|---|---|---|
| 200x100 x20x2,5 | 8,27 | 1,05 | 31,5 | 6,9 | 69 | 80,9 | 1,37 | 20 | 36 | 2,1 |
| 3 | 9,84 | 1,25 | 31,4 | 8,14 | 81,4 | 80,6 | 1,6 | 23,3 | 35,7 | 3,76 |
| 3,5 | 11,4 | 1,45 | 31,4 | 9,34 | 93,4 | 80,3 | 1,82 | 26,5 | 35,4 | 5,92 |
| 4,5 | 14,4 | 1,83 | 31,2 | 11,6 | 116 | 79,6 | 2,21 | 32,1 | 34,7 | 12,3 |
| | | | | | | | | | | |
| 225x75 x20x2,5 | 7,78 | 0,991 | 20,6 | 7,49 | 66,6 | 86,9 | 0,701 | 12,9 | 26,6 | 2,06 |
| 3 | 9,25 | 1,18 | 20,5 | 8,83 | 78,4 | 86,6 | 0,814 | 14,9 | 26,3 | 3,53 |
| 3,5 | 10,7 | 1,36 | 20,5 | 10,1 | 89,9 | 86,2 | 0,919 | 16,9 | 26 | 5,56 |
| 4,5 | 13,5 | 1,72 | 20,4 | 12,5 | 111 | 85,4 | 1,1 | 20,2 | 25,3 | 11,6 |
| | | | | | | | | | | |
| 225x100 x20x2,5 | 8,76 | 1,12 | 29,8 | 9,04 | 80,3 | 90 | 1,42 | 20,3 | 35,7 | 2,33 |
| 3 | 10,4 | 1,33 | 29,7 | 10,7 | 94,9 | 89,6 | 1,66 | 23,7 | 35,4 | 3,98 |
| 3,5 | 12,1 | 1,54 | 29,7 | 12,3 | 109 | 89,3 | 1,89 | 26,8 | 35,1 | 6,27 |
| 4,5 | 15,2 | 1,94 | 29,5 | 15,2 | 136 | 88,6 | 2,3 | 32,6 | 34,4 | 13,1 |
| | | | | | | | | | | |
| 250x65 x20x2,5 | 6,36 | 0,81 | 16,2 | 7,2 | 57,6 | 94,3 | 0,421 | 8,62 | 22,8 | 1,08 |
| 3 | 7,88 | 1 | 16,2 | 8,84 | 70,7 | 93,9 | 0,508 | 10,4 | 22,5 | 2,09 |
| 3,5 | 9,37 | 1,19 | 16,1 | 10,4 | 83,3 | 93,4 | 0,588 | 12 | 22,2 | 3,58 |
| | | | | | | | | | | |
| 250x75 x20x2,5 | 8,27 | 1,05 | 19,4 | 9,61 | 76,9 | 95,5 | 0,723 | 13 | 26,2 | 2,19 |
| 3 | 9,84 | 1,25 | 19,4 | 11,3 | 90,7 | 95,1 | 0,839 | 15,1 | 25,9 | 3,76 |
| 3,5 | 11,4 | 1,45 | 19,4 | 13 | 104 | 94,7 | 0,948 | 17 | 25,6 | 5,92 |
| 4,5 | 14,4 | 1,83 | 19,3 | 16,1 | 29 | 93,9 | 1,14 | 20,4 | 24,9 | 12,3 |

Figure 22: Lip channel data from Tubecon

| Lip Channel Dimensions | | | Standard Material and Wall Thickness* | | |
|---|---|---|---|---|---|
| Width | Height | Lip | SAE1008 | S355 | Z275 (Pre-Galv) |
| 75 | 45 | 15 | 2mm-4mm | 2.5mm-4mm | 2mm |
| 75 | 50 | 20 | 2mm-4mm | 2.5mm-4mm | 2mm |
| 100 | 50 | 20 | 2mm-4mm | 2.5mm-4mm | 2mm |
| 125 | 50 | 20 | 2mm-4mm | 2.5mm-4mm | 2mm |
| 125 | 65 | 20 | 2mm-4mm | 2.5mm-4mm | 2mm |
| 125 | 75 | 20 | 2mm-4mm | 2.5mm-4mm | 2mm |
| 150 | 50 | 20 | 2mm-4mm | 2.5mm-4mm | 2mm |
| 150 | 75 | 20 | 2mm-4mm | 2.5mm-4mm | 2mm |
| 175 | 50 | 20 | 2mm-4mm | 2.5mm-4mm | 2mm |
| 175 | 75 | 20 | 2mm-4mm | 2.5mm-4mm | 2mm |
| 200 | 50 | 20 | 2mm-4mm | 2.5mm-4mm | 2mm |
| 200 | 75 | 20 | 2mm-4mm | 2.5mm-4mm | 2mm |
| 225 | 50 | 20 | 2mm-4mm | 2.5mm-4mm | 2mm |
| 225 | 75 | 20 | 2mm-4mm | 2.5mm-4mm | 2mm |
| 250 | 50 | 20 | 2mm-4mm | 2.5mm-4mm | 2mm |
| 250 | 75 | 20 | 2mm-4mm | 2.5mm-4mm | 2mm |
| 300 | 50 | 20 | 2mm-4mm | 2.5mm-4mm | 2mm |
| 300 | 75 | 20 | 2mm-4mm | 2.5mm-4mm | 2mm |
| 100 | 65 | 15 | 2mm-4mm | 2.5mm-4mm | 2mm |
| 150 | 65 | 20 | 2mm-4mm | 2.5mm-4mm | 2mm |
| 175 | 65 | 20 | 2mm-4mm | 2.5mm-4mm | 2mm |
| 200 | 65 | 20 | 2mm-4mm | 2.5mm-4mm | 2mm |
| 225 | 65 | 20 | 2mm-4mm | 2.5mm-4mm | 2mm |
| 250 | 65 | 20 | 2mm-4mm | 2.5mm-4mm | 2mm |
| 300 | 65 | 20 | 2mm-4mm | 2.5mm-4mm | 2mm |

Figure 23: Lips and open channel data from Tubcon

After analysing and studying data from a various company, data from Tubecon company (shown in figure 23) was selected with web length 250mm, flange length 65mm, lip length 20mm, and thickness 2 mm is considered for the dimension of channel and zed section beam for the geometry of FE model.

### 3.2.2 Spam length of the beam

FE model of C and Z section beam testing will be conducted with different spam lengths, it will help to study and understand the behavior of reaction force due to different spam lengths. First, the channel beam with a large spam length of 4200mm will be considered from the previously performed experiment at the University of the Strathclyde, and second will be the shortest random selected spam length of 1000mm for innovation and Maintaining creativity of the thesis for analysis of pure bending. To avoid confusion between the innovation model, let assumed that Model-alpha to FE innovation channel beam and Model-beta to FE innovation zed beam.

### 3.2.3 Bolts holes

The overall height of the channel and Zed section is 250mm. Holes for bolts connection are needed to be calculated through an equal distance of height from the neutral axis of the beam (shown in bottom figure 8). Where holes diameter should be drawn between18mm to 22mm for nominal section size of 250mm to 350mm. A diameter of 20mm is used in hole dimension ($D_H$) for the FE model.

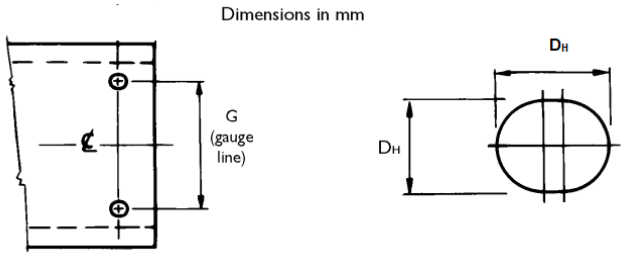


Figure 24: Bluescope Lysaght company punching holes

### 3.2.4 Loads on overall bolts length

The axial bolt force, which is the primary load in the bolt up condition, is used to clamp the web, to acquire the initial seal, the sufficient load should be provided and this seal should remain long-term for the joint's life and to overcome the obstacles, there should be a necessary safety factor for the load which is greater than required. Force impacts will affect the flange performance, stress distribution near holes, axial shift, and flange rotations.

While performing a pure bending test, a Maximum amount of reaction force will be generated near the support members. Beams and support members are connected through the nuts and bolts, there are absolute changes in the development of higher shear stress in overall bolt length due to vertical load generated from flange thickness and it will be much higher for each stage of incrementing displacement in a downwards direction at Y-axis.

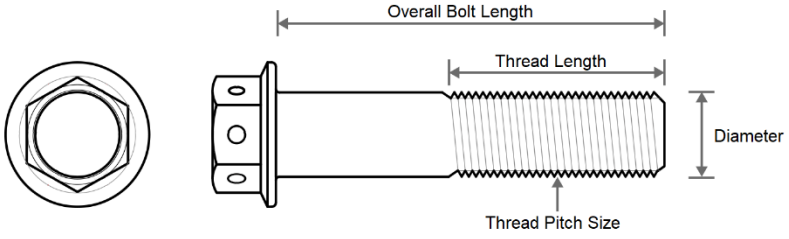


Figure 25: Bolt and nut diagram

## 3.3 Summary

The design and Analysis chapter has provided rational information on the safe practice of design and selecting the proper dimension. The inaccurate result is the product of less consideration regarding design and loading conditions near connection between two bodies.

Various types of uncertainty in design and loading conditions can affect the performance of the channel and zed beam during the bending test. This chapter has to gather valid informative data regarding performing design sketches in AutoCAD. All dimensional data for beam are collected through an industrial website and testing has already been performed.

# Chapter 4 (Development of finite element c and z model)

## 4.1 Introduction

Two different dimensional FE model is used for Channel beam bending test, the first channel is used for setup non-linear analysis and also to understand parametric setting used during simulation in Ansys. all dimensional and verification of data are gathered from previous lab experiments performed at the University of the Strathclyde. The same dimension of channel beam, support block, and loading block is used for the creation of the FE model from starch in Ansys. The same non-linear material properties were used during the simulation of all the FE models.

Second channel section dimensions are selected from Tubecon company for the creation of innovation FE model - A; the difference between the first and second channel beam is span length. The same parametric setting is used to simulate the second channel beam. zed section beam data are also collected from Tubecon company and similarly, the same parametric setting is used to simulate zed beams (Innovation FE model – B).

## 4.2 Geometry and Material properties.

Geometry and material properties are collected from a lab channel beam experiment performed at the University of Strathclyde for a three-point bending test (shown in bottom table1, table 2, table3, and table 4).

Table 1: Experimental channel section beam dimension

| **Channel Section Dimension** | |
|---|---|
| Web | 141.63mm |
| Flange | 52.90mm |
| Lip | 18.55mm |
| Thickness | 1.56mm |
| Fillet Radius | 2mm |
| Section span | 2400mm |

Table 2: Support block members dimension

| **Support Block Dimension** | |
|---|---|
| Length | 140mm |
| Width | 50mm |
| Height | 191.63mm (25mm above & below channel section) |

Table 3: Loading block member dimension

| Loading block | |
|---|---|
| Length | 120mm |
| Width | 50mm |
| Thickness | 25mm |

Table 4: Non-linear material properties

| Non-linear Material properties | |
|---|---|
| Young's modulus (E) | 203Gpa |
| Yield strength | 390Mpa |
| Poisson Ratio (V) | 0.3 |

The model was designed in Ansys and assigning material properties from table 4, university lab experiment data are used for channel beam (shown in table 1), support block members in blue colour (shown in bottom figure 26) are drawn using data from table 2, Loading block is represented in red colour (shown in figure 27) and dimensions are given in table 3.

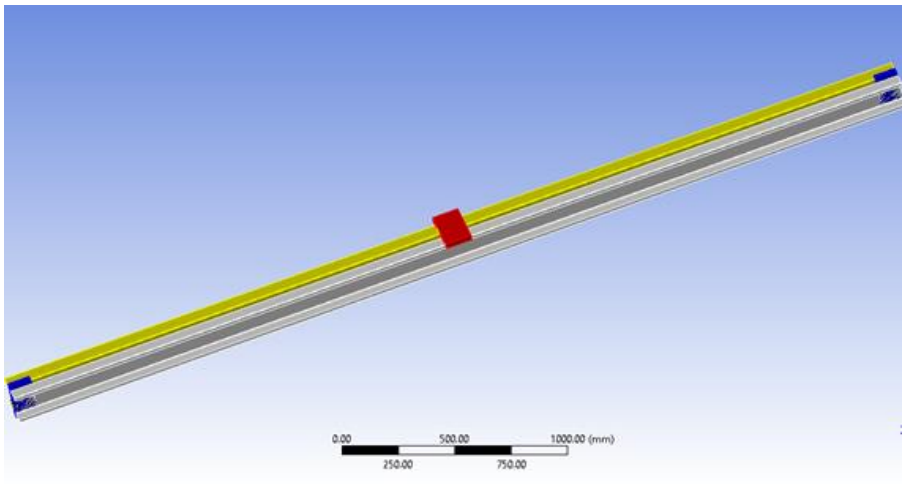


Figure 26: Channel 3-point bending test setup.

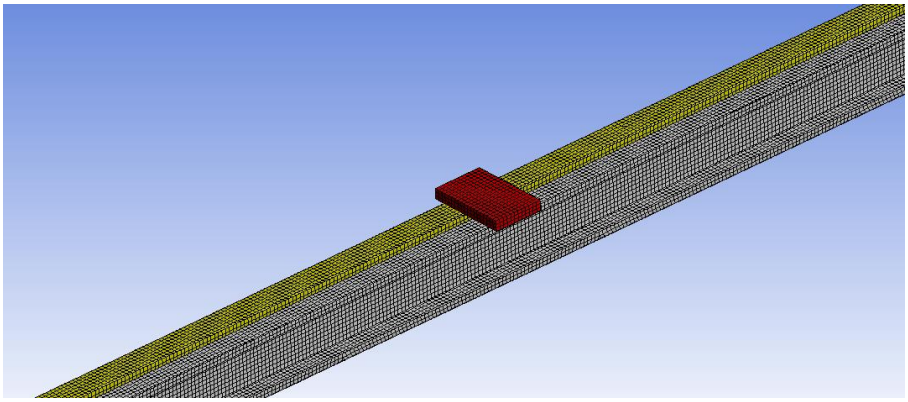

Figure 27: Isometric view of Loading block in centre of the beam

## 4.3 Brief details on the sketch of the C section and Z section

The Geometry of the C and Z section beam is drawn in design modular, the designing process is divided into two-stage. Firstly, the cross-section of the channel is coded into finite length. the sketch of C and Z includes flange length, depth (height of channel), lips length, and radius, was drawn in the “LINE” sketch method in 2D (XY plane) to achieve shell types elements (shown in bottom figure 28).

The unit is set in millimeters (mm). Secondly, spam is created from the same sketch of the beam and it is possible through the extended length of 1000mm into Z directional plane. Add material operation is selected in extrude method without considering thickness for the formation of shell structure model.

Thickness is not essential for shell elements but thickness mode can be assigned later in the cross-sectional area of the beam, after successful completion of the overall model in the form of the surface body. The thickness mode is set in “user define” and values of 1mm, 1.5mm, 2mm, 3mm, and 4mm are considered in experiments.

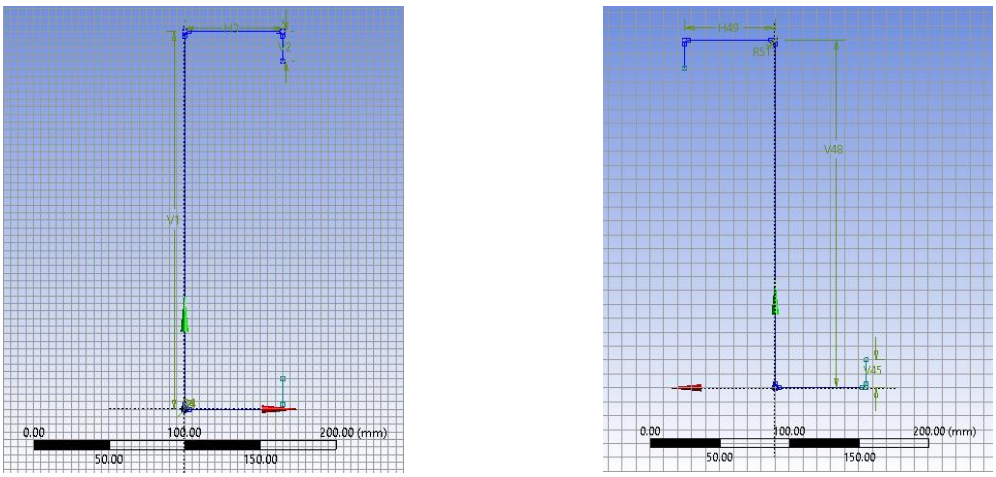


(a) (b)

Figure 28: (a) & (b) Line sketch of C and Z section

C and Z sections are manufactured using curved portion known as fillets, it is the transition between flange and webs, as well as lips and flange. The four small fillets or round corner designs to joined webs, flange and lips together to form an open section structural profile, with a defined fillet radius of 3mm (shown in figure 29)

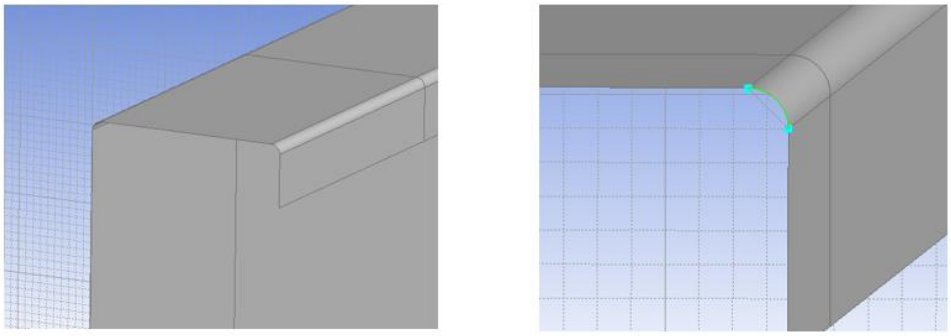

Figure 29: Fillet section

The splitting face method is used to improve the efficiency of surface contacts and joints between beam and block, which are among the connection parameters. The channel beam is split into 45 faces using the split face method (shown in figure 30) and similarly, the zed beam has split into 23 faces (shown in figure 31). Three solid blocks are placed near the C and Z model with a gap of 0.001mm. Two identical blocks are bolted to the back surface of the beam to provide fixed support parameters, and the upper block is located in the middle of the beam to develop a central load case situation.

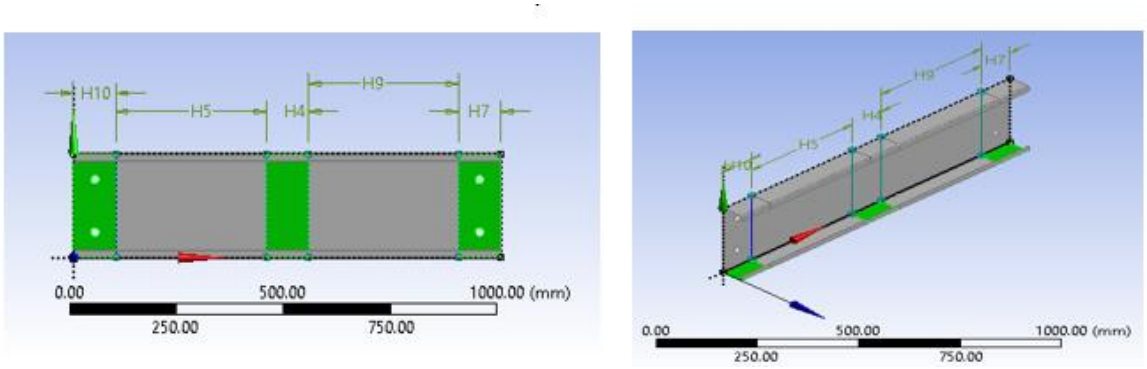


Figure 30: Channel beam split face diagram

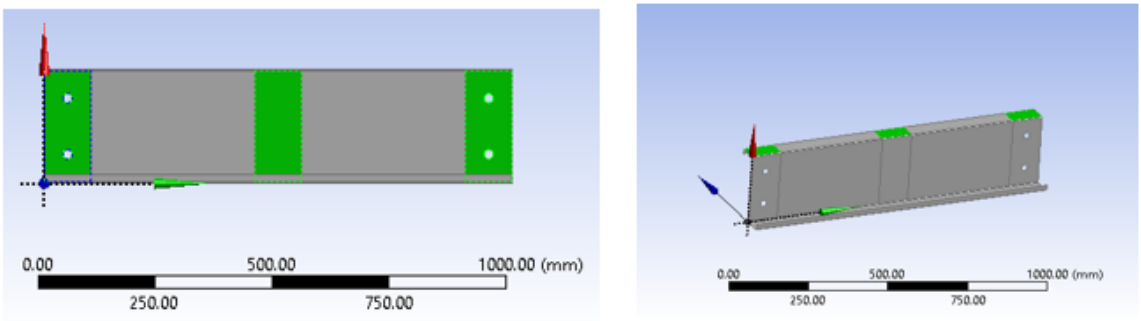


Figure 31: Zed beam split face diagram

## 4.4 Channel beam support member blocks

Support blocks in the channel beam provide a fixed support case for analysis. blocks are 900mm apart from their neutral axis (shown in figure 32), the height of the block is 300mm (25mm above and 25mm below the 250mm channel height), the width of the block is 100mm, and thickness of the block 25mm. The block is drawn from the new generate plane parameter near the channel section, new XYZ plane has been transformed 1 (RMB) with an offset of -0.001mm applied in the x-axis to make a gap of 0.001mm between channel surface and block surface (shown in figure 33). transform 2 (RMB) with an offset of -25mm applied in the y-axis to ease the drawing location with higher accuracy for block members and also to achieve 25mm height below the channel.

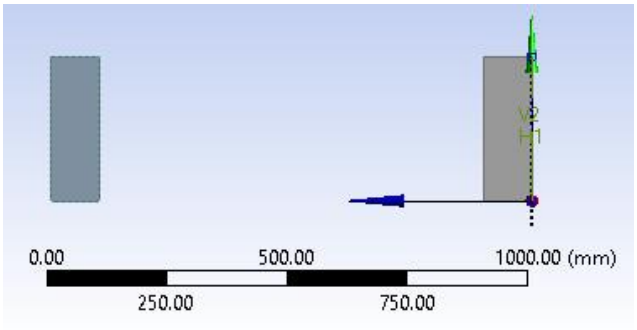


Figure 32: Distance between two support blocks

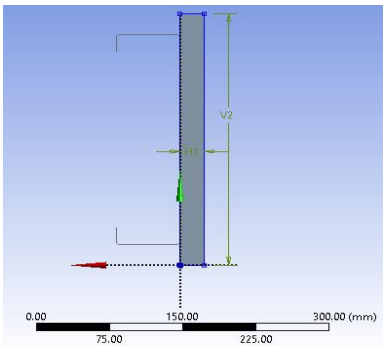


Figure 33: channel and block configuration

Holes in support blocks are generated through the creation of new XY planes on top of extruding length (width) of 100mm. The diameter of the holes is 20mm and the Split face area on the channel beam provides the perfect contact surface between the channel surface and block surface (shown in figure 34).

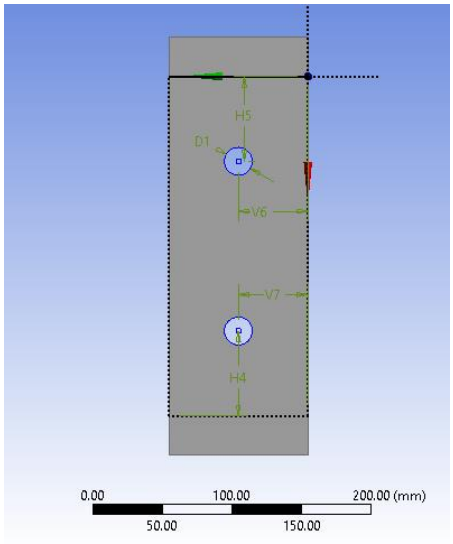


Figure 34: Support block split face diagram

## 4.5 Zed beam support member blocks

Support block members of the zed section beam are also for a fixed support case study. blocks are 900mm apart from their centerline of the holes (shown in figure 35), the height of the block is 226.5mm, the width of the block is 100mm, and the thickness of the block 25mm (shown in figure36). The two-block is drawn separately from two different generate planes near the end of the zed beam.

Support block A - XYZ plane has been transformed 1 (RMB) with an offset of 0.001mm applied in the x-axis (0.001mm is the gap between block and zed surface) and transform 2 (RMB) with an offset of -10mm applied in the y-axis (10mm is the clearance gap).

Similarly, block B – XYZ plane has been transformed 1 (RBM) with an offset of 1000mm in the z-axis, transform 2 (RMB) with an offset of -10mm applied in the y-axis, and transform 3 (RMB) with an offset of 0.001mm applied in the x-axis.

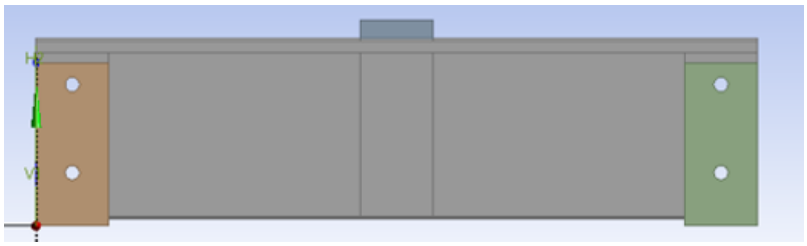

Figure 35: Distance between block A & block B diagram

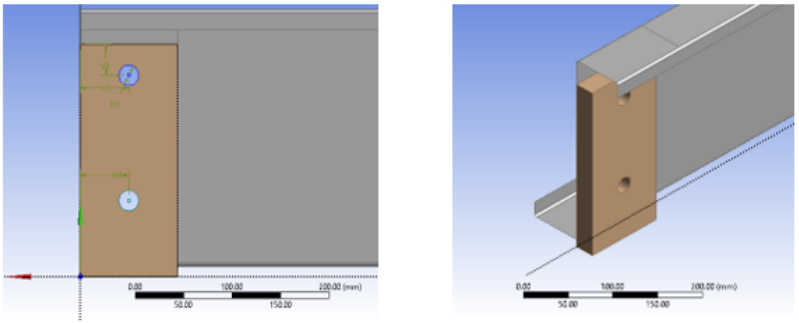

Figure 36:Support block configuration

## 4.6 Loading block member

The top-loading block of the C beam has a length of 200mm, width 100mm, and thickness of 25mm but for the Z beam was half the length (L/2), width (W/2), and thickness remain constant (25mm). new XYZ plane is created near channel beam with transform 1 (RMB) offset of 500mm in the z-axis (which will transfer sketch coordination parameter in the middle of the beam), sketch plane has now been shifted to the middle of the beam and similarly transform 2 (RBM) with an offset of 250mm in the y-axis (It will shift the sketch coordination parameter 250mm above the beam). For Channel beam transform 3 (RBM) offset value of -13.5mm in the x-axis (It will shift the sketch coordination parameter in the middle of the two-channel beam – shown in figure 37) but for Zed beam transform 3 (RBM) offset value is zero. Add material operation has been applied into extrude process with the both-symmetrical direction of 50mm to make the width of 100mm (shown in figure 38).

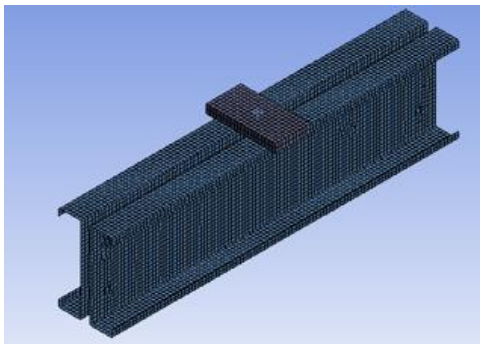

Figure 37: Channel beam loading block configuration

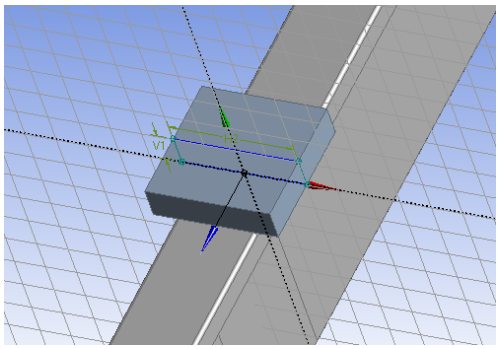

Figure 38: Zed beam loading block configuration

20000mm$^2$ surface area of loading block has been divided into two equal parts through the split face (shown in figure 39), each part of the surface contain the area of 10000mm$^2$. It provides an accurate contact region and also avoids overlapping distribution area into the channel bending beam model (shown in figure 30). No modifications are applied to the Zed beam bending model.

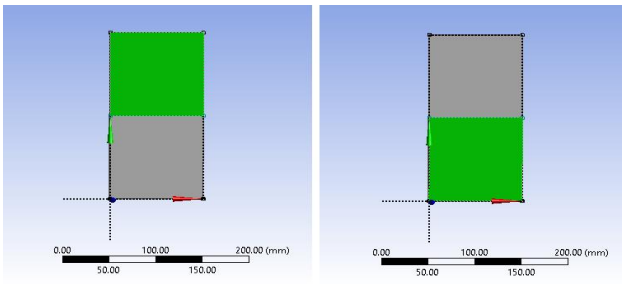


Figure 39: loading block split surfaces

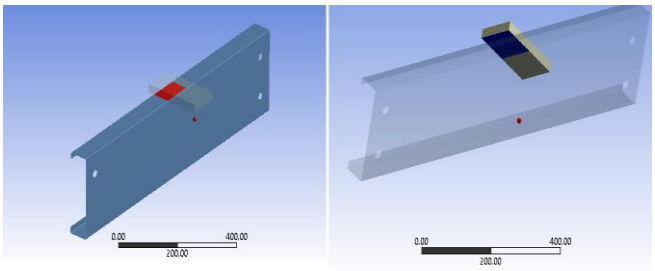


Figure 40: Two contact region in channel loading block

## 4.7 Meshing and Element types

The thin walls of the Channel section area have meshed with shell elements, which are well known for their performance regarding faster convergence in dealing with thin-walled structures. This is possible through automatic model meshing in Ansys.

SHELL 281 elements are selected for large strain non-linear analyses. shell thickness effect is also a consideration. The element accounts for distributed pressure follower (load stiffness) effects. SHELL 281 is suitable for analysing thin to moderately thick shell structures. The element has an 8-node quadrilateral finite shape with six degrees of freedom at each node; translations in the x, y, and z axes, and rotations about the x, y, and z-axes.

The body sizing and edge sizing mesh method are appointed in the surface body and element size is set to 10mm. it is observed that the total number of 27,049 nodes and 8,817 elements has been generated (shown in figures 41 & 42).

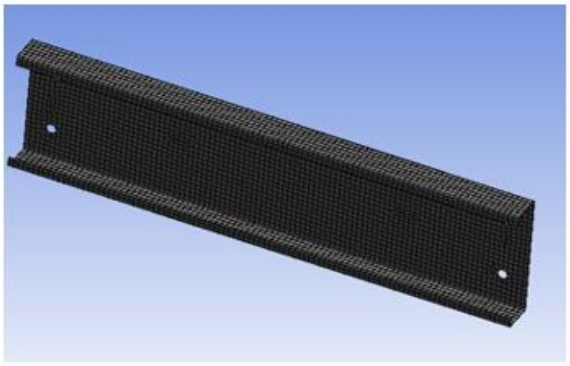

Figure 41: single-channel mesh Figure

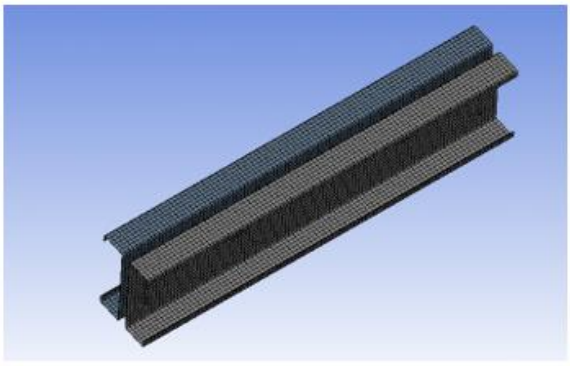

42: double channel beam mesh

The side support structure and top-loading structure are mesh using SOLID 186, It is 3D elements that have a higher order of 20-node that exhibits quadratic displacement behavior. The element is defined by 20 nodes having three degrees of freedom per node: translations in the nodal x, y, and z-directions.

The element supports plasticity, hyper-elasticity, creep, stress stiffening, large deflection, and large strain capabilities. It also has mixed formulation capability for simulating deformations of nearly incompressible elastoplastic materials, and fully incompressible hyperplastic materials. Similarly, the body sizing and edge sizing mesh method are appointed in three solid block members, and element size is set to 10mm. it is observed that the total number of 1,809 nodes and 10,010 elements has been generated on the side support block. Where the top load structure contains 3,337 nodes and 600 elements. (Shown in figure 43 & 44)

Overall statics for selecting shell and solid body component together and generating mesh through appointing quadratic element order with body sizing method, inputting user define the value of 10mm elements size, provides the result with 40,396 nodes and 11,226 elements.

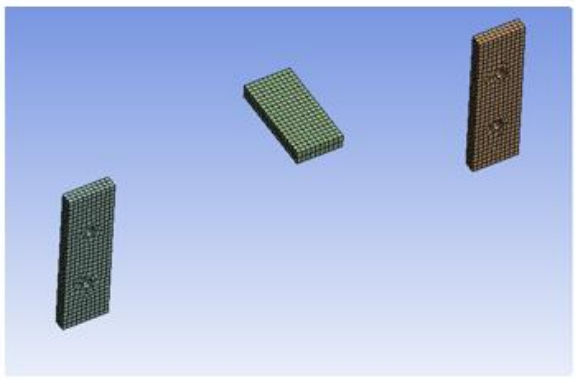

Figure 43: loading and side support members mesh

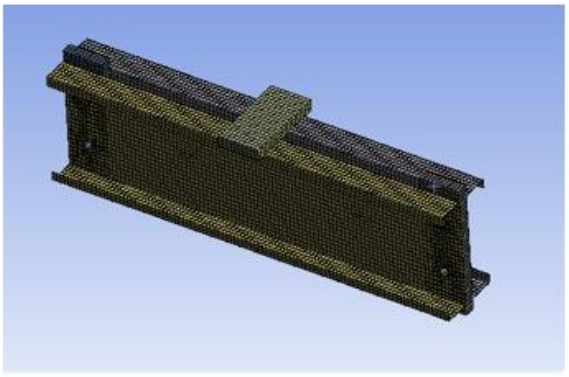

Figure 44: Overall mesh diagram of channel beam

Similarly, the Zed beam area also formed using SHELL 281 elements for non-linear analysis. The body sizing and edge sizing mesh method are assigned to the surface body (Zed beam) and the mesh element size is 10mm (shown in figure 46). the efficient solution comes from accurate meshing; quadrilateral elements order is performed to generate structural mesh because the concept of structural mesh in the model is to simplify the model in the right way to achieve accurate analyses. it is observed that the overall static of surface and solid body has some 22,520 nodes and 5,988 elements (shown in figure 45).

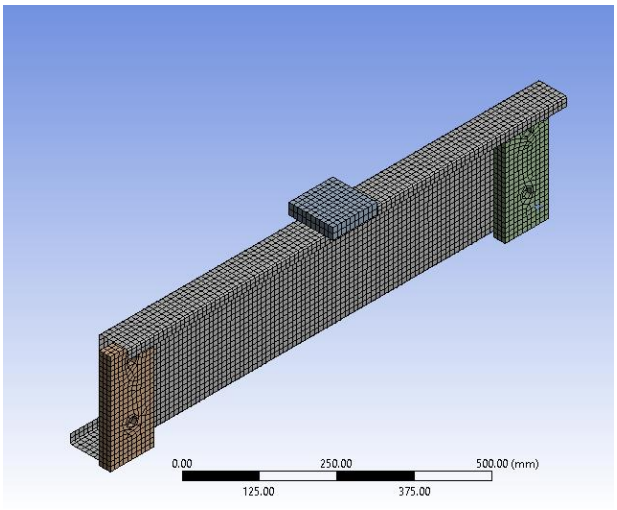


Figure 45: Overall mesh diagram of Z beam

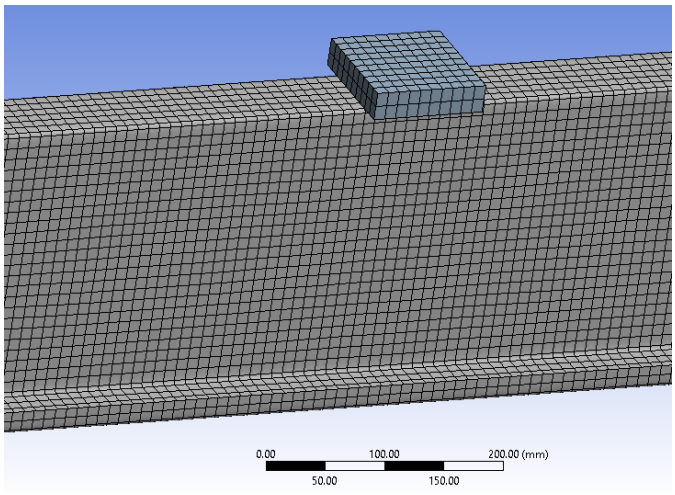


Figure 46: mesh element size 10mm

## 4.8 Verification of meshing quality

Mesh quality verification was performed through skewness number and orthogonality checking, designers highly suggest a low orthogonal quality or high rates of skewness. (shown in bottom figure 47)

**Skewness** mesh metrics spectrum

| Excellent | Very good | Good | Acceptable | Bad | Unacceptable |
|---|---|---|---|---|---|
| 0-0.25 | 0.25-0.50 | 0.50-0.80 | 0.80-0.94 | 0.95-0.97 | 0.98-1.00 |

**Orthogonal Quality** mesh metrics spectrum

| Unacceptable | Bad | Acceptable | Good | Very good | Excellent |
|---|---|---|---|---|---|
| 0-0.001 | 0.001-0.14 | 0.15-0.20 | 0.20-0.69 | 0.70-0.95 | 0.95-1.00 |

Figure 47: Mesh quality spectrum

### 4.8.1 Skewness ratio

In general, Skewness number is the major element quality factor that is being used in meshing structures, and maintaining the skewness ratio of the cell is the key factor to maintain quality in working with complex geometry.

Quadrilateral elements shape order is approached for structural mesh. A lower value of the ratio between the number of elements versus element metrics determines the high-quality skewness factor and skewness numbers between 0.00 to 0.25 are considered as excellent quality, total skewness of channel beam, support block, and top-loading block has a higher order of Quad8 and Hex20 elements. It maximum deviations of skewness order is 0.0328, which fall between 0.00 to 0.20, which indicates that the channel testing model has qualified the verification of skewness quality factor and few Tri16 has been observed due to triangular shape element because of same node number used twice to create triangle shape in meshing near holes of channel beam and support blocks. (shown in top figure 47)

e

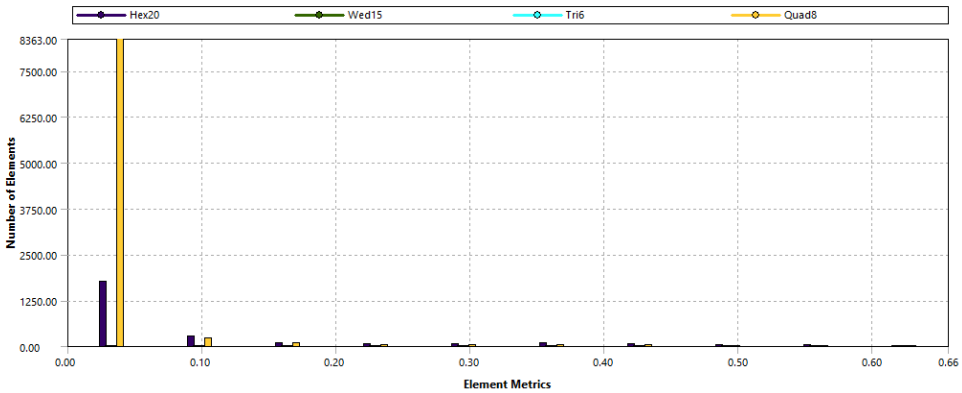


Figure 48: Channel beam skewness verification graph

Similarly, the Zed section beam, support block, and top-loading block are meshed together. Higher-order of Quad8 and Hex20 has been observed in skewness factor analysis and the maximum value obtained is 0, which falls between 0.00 to 0.10. hence, it indicates that the Zed testing model has qualified the verification of the skewness quality factor. (shown in top figure 47)

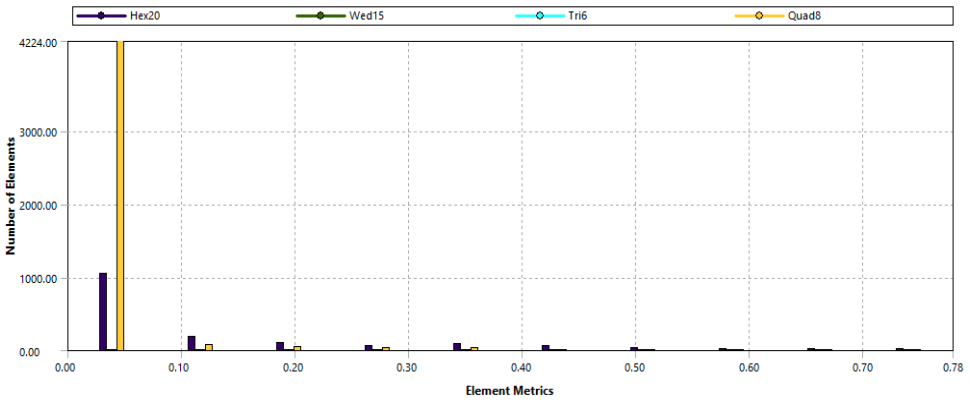


Figure 49: Zed beam skewness verification graph

### 4.8.2 Orthogonal quality

The mesh metric spectrum chart shown in the above figure is used to determine the quality of orthogonality. The concept of mesh orthogonality verification is to represent, how close the angle between two adjacent element faces or edges is to a certain optimal angle. For an effective solution, orthogonality efficiency for structure analysis should be greater than 0.60. Channel beam elements have developed Quad8 and Hex20 elements with an orthogonality of 0.975. Which fall under 0.90 to 1.00. hence, it can be said that mesh is shown to have qualified the orthogonality verification. (shown in top figure 47)

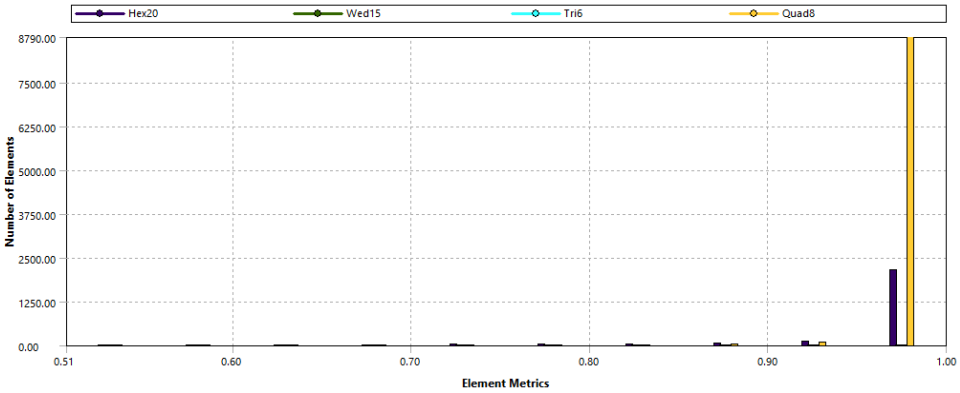


Figure 50: Channel beam orthogonal verification graph

Similarly, Zed section beam meshing verification quality has been carried through orthogonality. mesh elements have developed Quad8 and Hex20 elements with an orthogonality of 0.976. Which fall under 0.90 to 1.00. mesh has again qualified the orthogonality verification and it is acceptable for further process of simulation. (shown in top figure 47)

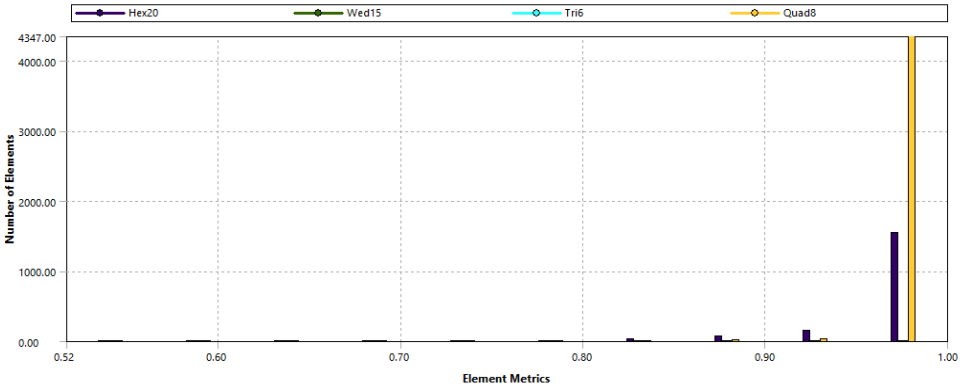


Figure 51: Zed beam orthogonal verification graph

# Chapter 5 (Model setup)

The model is designed for the simulation of a three-point bending test. the three-point bending configuration consists of two-channel section components that are back to back, with two fixed support blocks at each end. There is a third component in the middle, that will apply the loading to the parts.

## 5.1 Connection

### Surface Contacts and joints

Channel beam connection consists of contact surface and joints. Two support blocks are in frictional contact surfaces with opposite surfaces of the channel beam. The top-loading block is in bonded contact surface to avoid sliding of small block effect during simulation.

The split face on the channel beam provided efficient contact between block and surface. Highlighted red colours are contact face and blue colours are target face. The friction coefficient for frictional contact is 0.65 and normal stiffness factor is 0.2 (shown in figure 52 & 53).

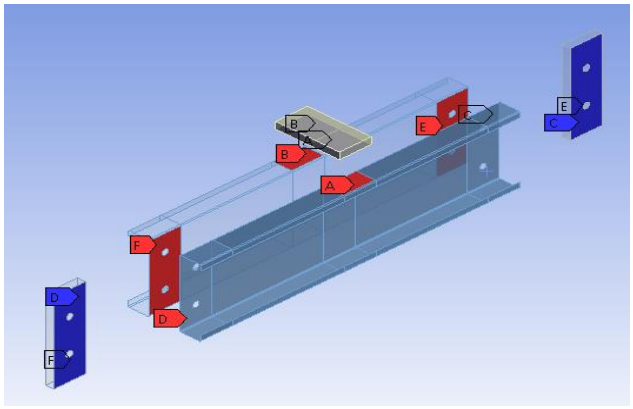

Figure 52: Overall contact surface in channel beam beam

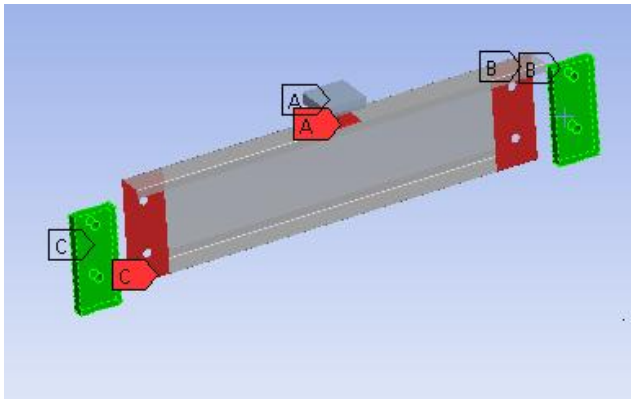

Figure 53: Overall contact surface in zed

Joints act as a connecting medium between beams and blocks. Fixed type with a body-to-body connection is used between the surface and solid model (shown in figure 54).

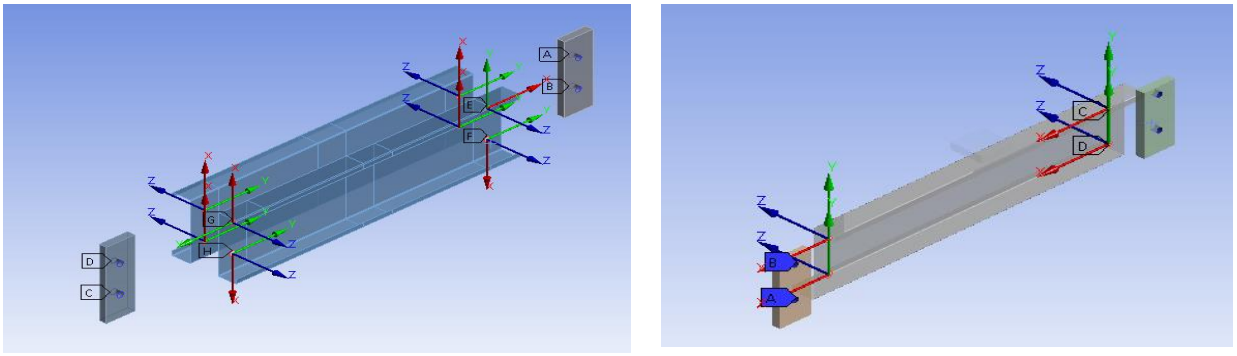

(a) (b)

Figure 54: (a) & (b) Overall joint between beam and support block members

## 5.2 Boundary and Loading condition

The support block is fixed in all degrees of freedom, the lower surface of the support blocks was restrained in translation, and the surface on the outside edge of the blocks was restrained in rotation. The loading blocks are restricted to only allowing y-axis translation. The top-loading block is applied with -10mm displacement in the y-axis, which allows the beam to generate the maximum amount of force in the y-axis (shown in figure 55).

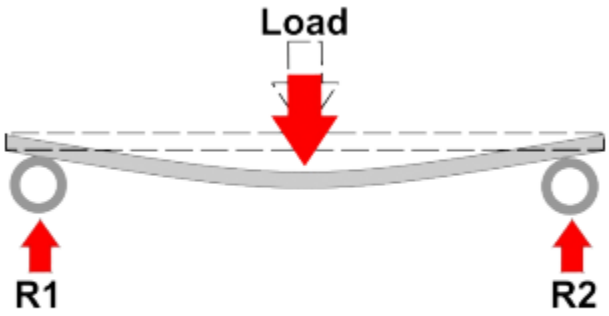


Figure 55: Three-point beam bending diagram

While performing maximum beam bending analysis, all downward forces are balanced by equal and opposite upward forces (Reaction force), where a beam is simply supported at each end and the beam is said to be kept in equilibrium. The bottom face of the support block in green colour (shown in figure 56 - a & b) is kept at fixed support mode in a static structure analysis setting.

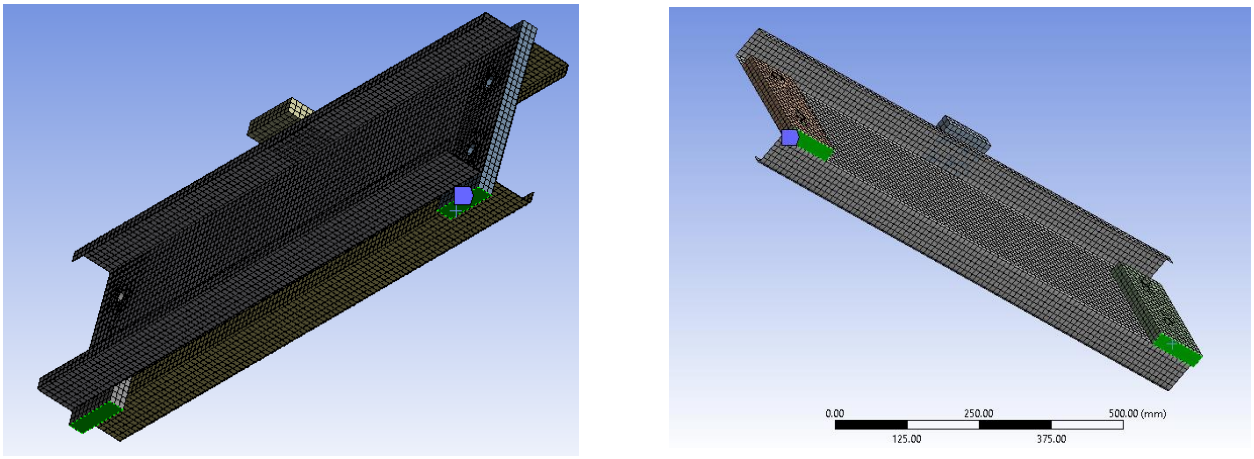


(a) (b)

Figure 56: Fixed support boundary condition in Z & C surface block of the beam

# Chapter 6 (Parametric study)

## 6.1 Three-point testing of Channel beam

The model was developed to simulate an experiment based on a three-point bending test. Research data are used from previous experiments performed by the Mechanical and Aerospace engineering department from the University of Strathclyde. The experiment data are used for only validation of the reaction force of the FE model.

The experiment is divided into two different Span lengths. The physical testing span used during the workshop experiment is 4200mm. First, finite element beam model dimension data are taken from experimental data (shown in table1, table2, table3 & table4) and second finite element Alpha-model span which is known as innovation channel model with span length of 1000mm and Third finite element Beta model which is also known as innovation zed model with a span length of 1000mm have identical dimension. such as the web height, flange length, lip length, and thickness. Data for FE alpha and FE beta model are taken from Tubecon company (shown in figure 22 & 23)

The yellow top block structure was loaded by applying a y-direction displacement to its top surface in a downward direction (shown in figure 57). Since it was consistent with the experimental procedure, the results were obtained from this central loading block. For each load step, the applied displacement and reaction force induced by the sections were both registered.

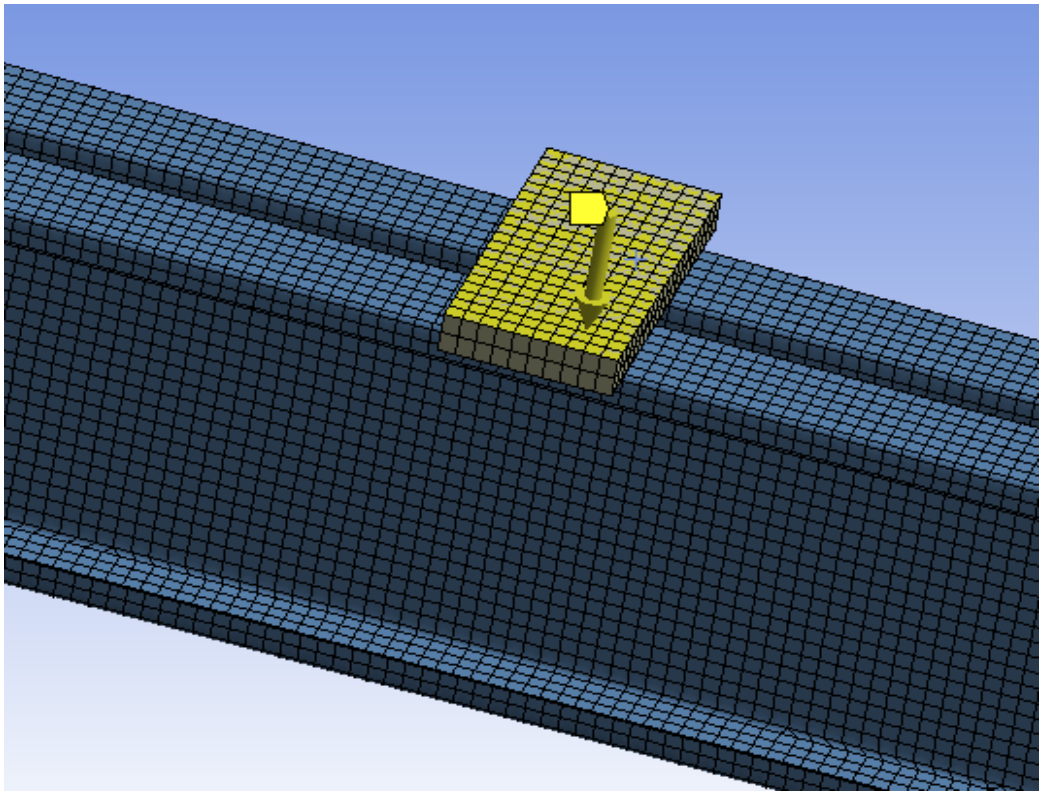

Figure 57: downward loading diagram

### 6.1.2 Result and verification

#### 6.1.2. (a) Channel section beam 1

The FE model simulation performance as a blue graph of applied displacement vs. reaction force at the loading block. The maximum load recorded on the channel section under experimental conditions is also indicated by the orange line in the graph (shown in figure 58).

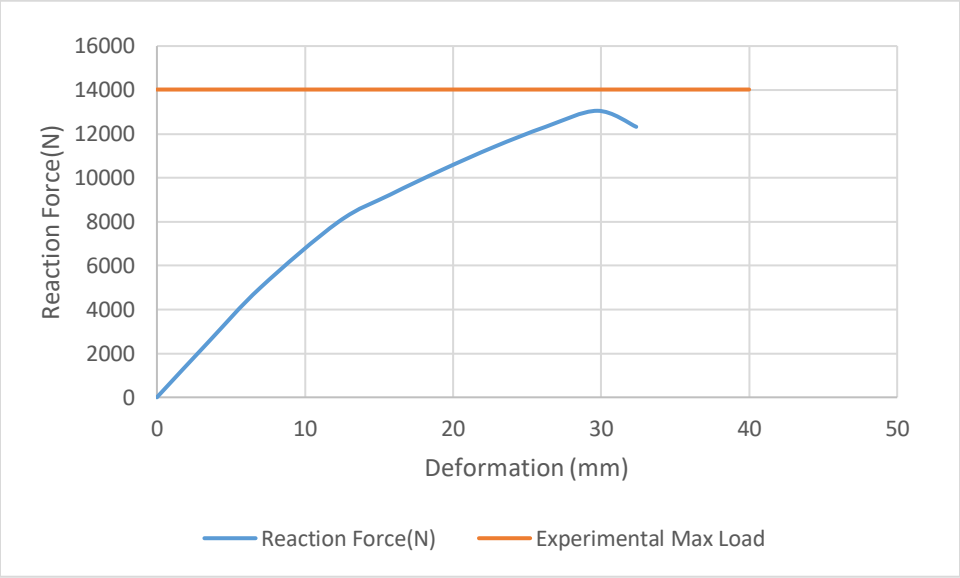


**Figure 58: Graph of 3-point bending test for FE deflection vs. reaction force**

In both cases, this force represents the maximum load the channel segment may withstand until web-crippling and plastic failure. The finite element method analysis gives a Maximum reaction force of 13.052KN and the Experimental method gives 14.020KN. The error between the FE and experimental results is 6.904% according to the bottom equation1 for error calculation, which indicates a clear comparison of the maximum load.

$$\boldsymbol{Error}\ \% = \left(1 - \frac{13.052}{14.020}\right) \times 100\% = 6.9044\% \qquad \ldots\ldots \textit{Equation 1: error \% calculation}$$

It must be observed that the stiffness of the model had a larger imbalance because it failed at a relatively low displacement than the experimental sections. This is considered to be caused in part to the connection providing a completely rigid connection. While the failure of the structure can address the uncertain behavior between the bolt and bolt hole.

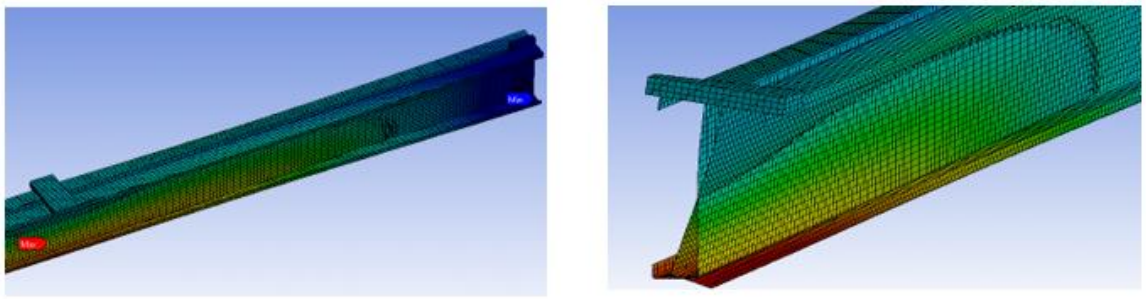

Figure 59: FE model simulation result of failure (section plane diagram)

### 6.1.2. (b) Channel section beam 2 (Innovation FE Alpha-model)

Since no experimental information was available for this design, a simulation was set up in a similar method performed for the above FE model with a 2400mm span. Innovation Alpha model is of 1000 mm span. The displacement is applied in Y-axis to generate a maximum amount of reaction force on the support block members.

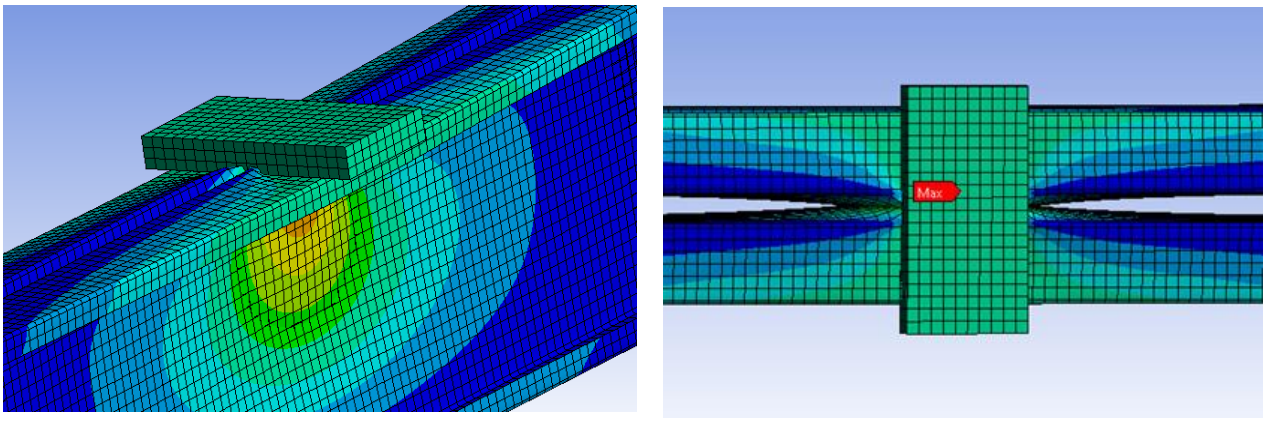


(a) Isometric view (b) Top view

Figure 60: (a) & (b) - deformation analysis near block and flange contact

The deformation of the channel beam has clearly shown in the above picture (figure 60); the maximum amount of bending stress has been induced in the middle of the section beam near the contact surface between the top-loading block and flange area of the beam. The beam web starts bending from the middle section members and maximum bending stress is gradually distributed around the middle area of the web. bending stress has to produce reaction force on support block members. The initial gap before the FE Alpha channel model experiment between the opposite side was 25mm. but after simulation, it has been observed that the gap between them is reduced near-neutral axis and surface near-neutral axis of the web are in mutual contact due to maximum equal bending stress distribution among both side of the channel beam and web crippling behavior has been observed (shown in figure 61)

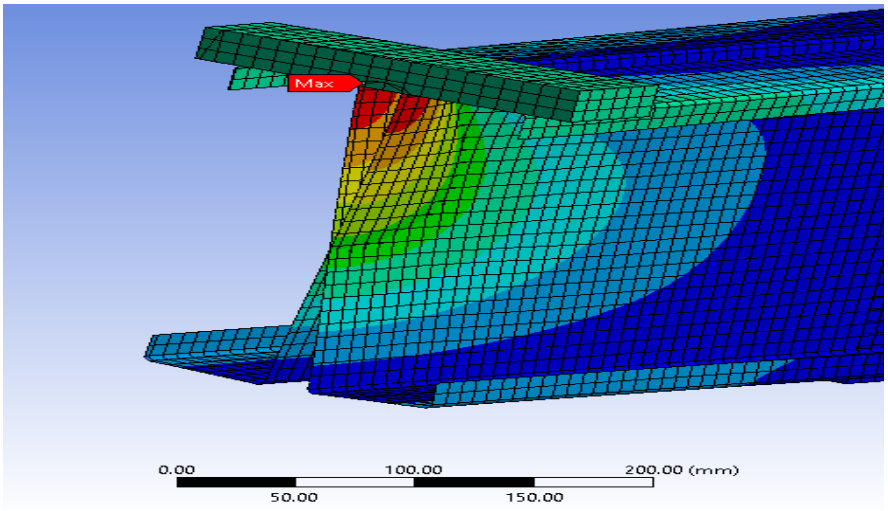


Figure 61: Sectional plane view for deformation

The result of the bending stress in the bottom figures is recorded from individual simulation of FE - Alpha (innovational model) and is shown in the blue graph of applied displacement vs. reaction force. The graph is plotted by performing 5 individual simulations with thickness range from 1mm, 1.5mm, 2mm, 3mm, and 4mm. It shows the change in reaction force for non-linear material after increasing thickness.

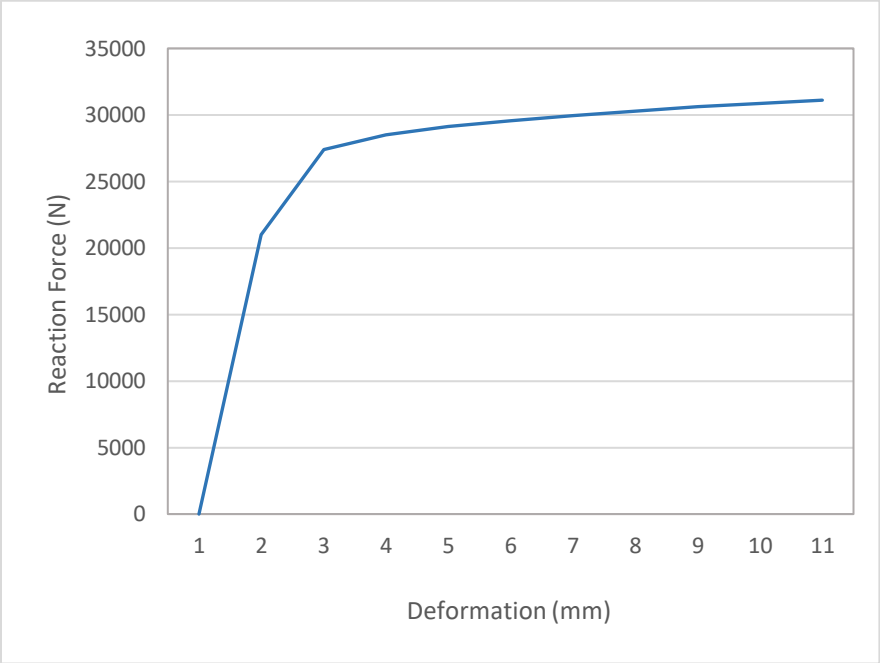


Figure 62: Alpha-model (Channel2) - Reaction force vs displacement (1mm thickness)

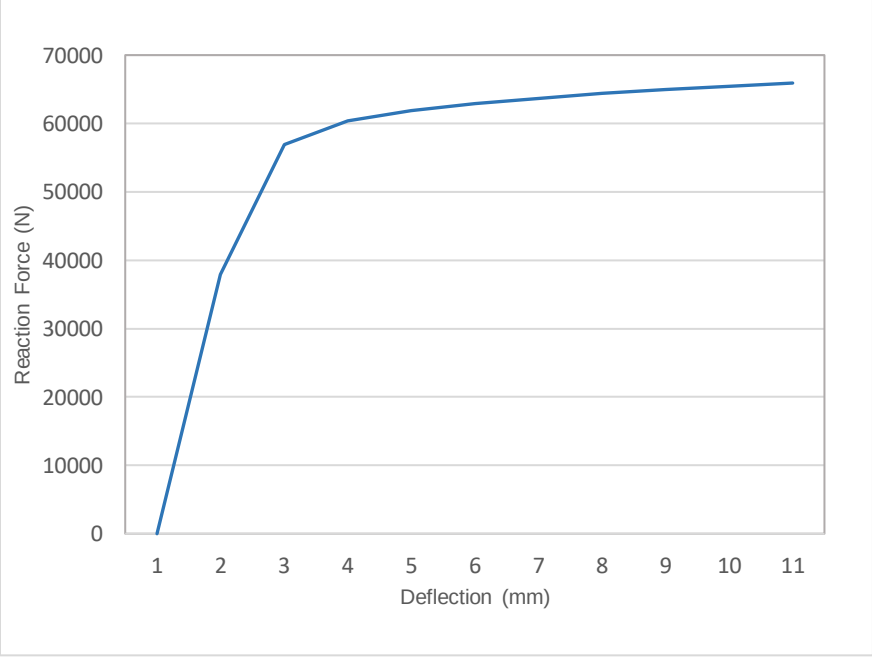


Figure 63: Alpha-model (Channel2) - Reaction force vs displacement (1.5mm thickness)

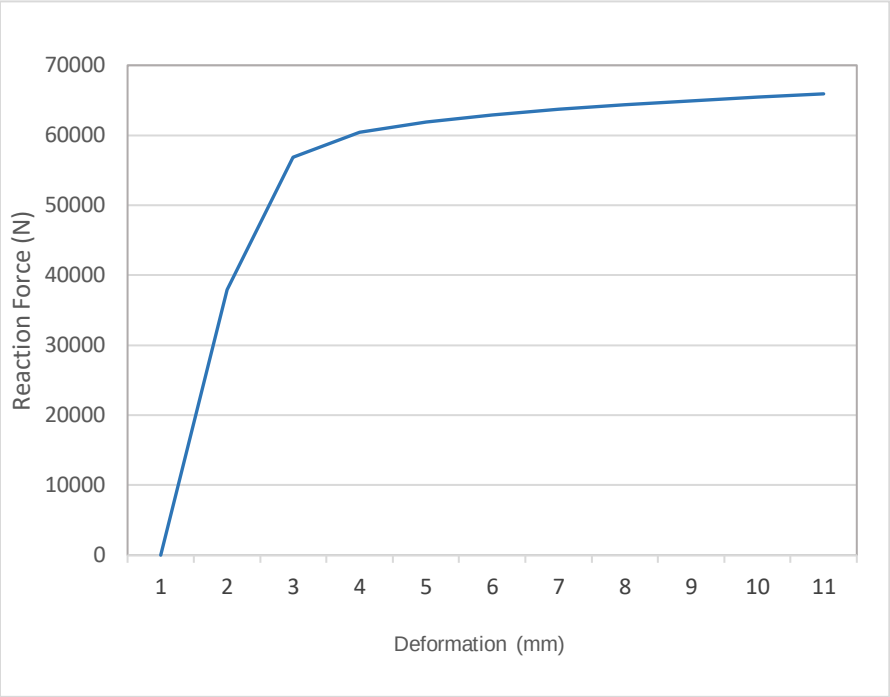


Figure 64: Alpha-model (Channel2) - Reaction force vs displacement (2mm thickness)

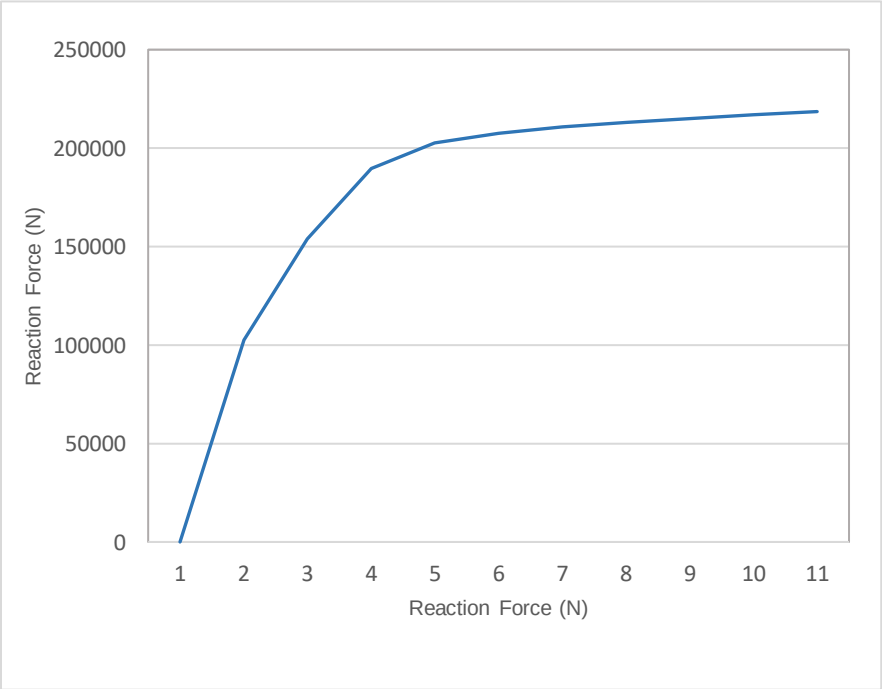


Figure 65: Alpha-model (Channel2) - Reaction force vs displacement (3mm thickness)

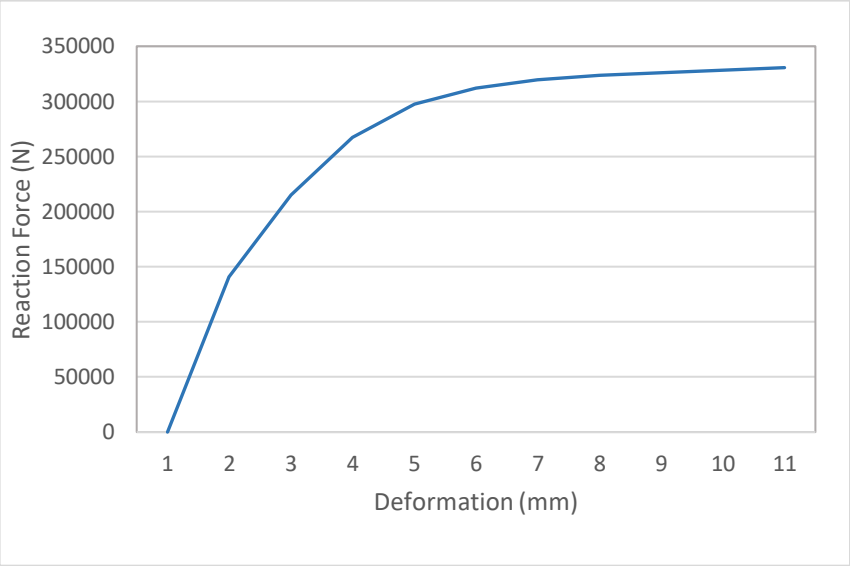


Figure 66: Alpha-model - Reaction force vs displacement (4mm thickness)

Table 5: Reaction force data of Alpha innovation model from different thickness

| Channel Section Thickness (mm) | Reaction Force (N) |
|---|---|
| 1 mm | 31112 N |
| 1.5 mm | 65918 N |
| 2 mm | 110050 N |
| 3 mm | 218560 N |
| 4 mm | 330600 N |

The individual simulation was performed, in variable thickness from 1mm to 4mm (shown in top table), to reproduce the testing conditions for validating the results, a parametric study was performed to measure the impact of undergoing different section thickness. the rate of change of maximum reaction forces is observed by increasing the section thickness. the result is shown in the form of a graph through plotting, the change in maximum reaction force supported by the section of the beam against the change in thickness (shown in table 5).

According to the graph, the data obtained from individual thickness simulation has shown the increases in reaction force. It can be said that supported block member has provided a large amount of support. no irregular or abrupt changes has been observed in maximum load between increasing variables, and they all obey the same linear trend (shown in figure 67).

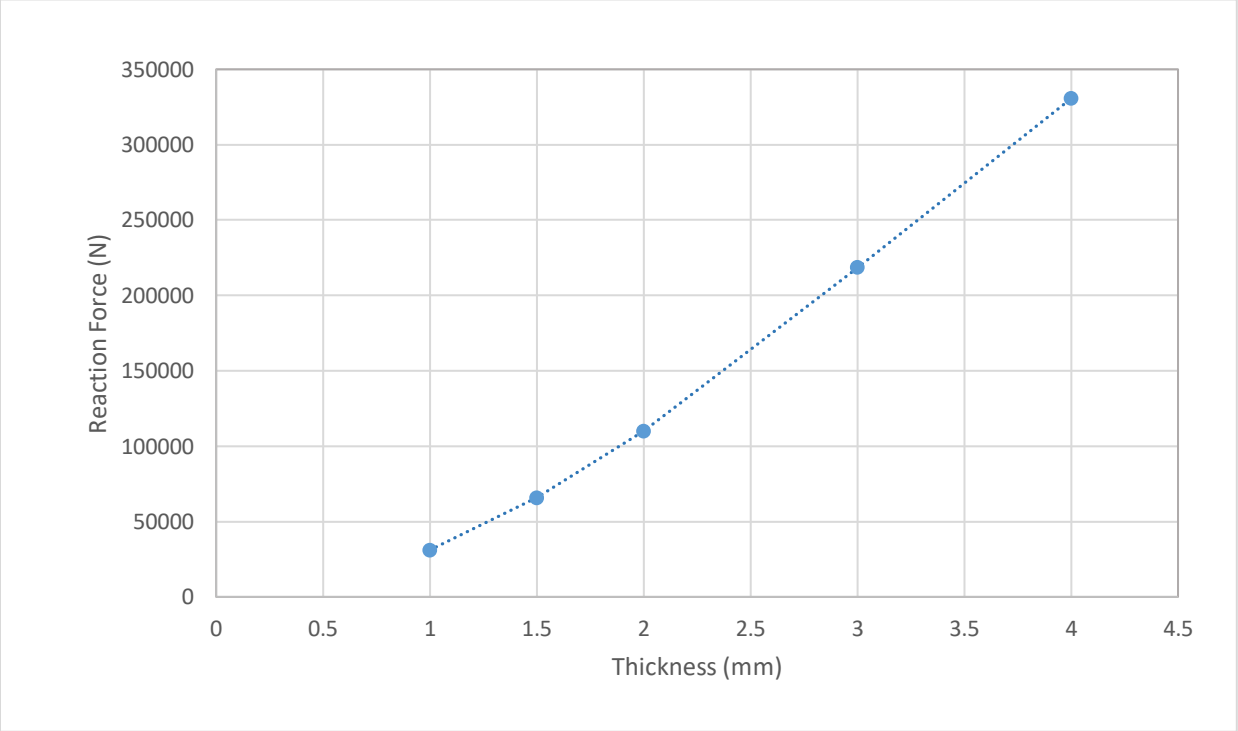


Figure 67: Alpha-model (Channel2) - reaction force vs thickness

All points are very close to the best-fit trend line. It is reasonable to assume that report results are reliable across a wide change in the spectrum of section thickness. This study has also demonstrated that the parametric study code tends to work as planned because the structure of an entire model was modified various times just by changing just one value for surface body thickness, and the data achieved were consistent in each test.

## 6.2 Three-point testing of Zed beam

The final element analysis techniques for zed sections are similar to the model setup used in the testing of both the channel beam. geometry, loads, and boundary conditions are all identical. Similarly, no experimental data were available for this design. displacement is applied in the y-axis to produce a maximum amount of reaction force on the support block members.

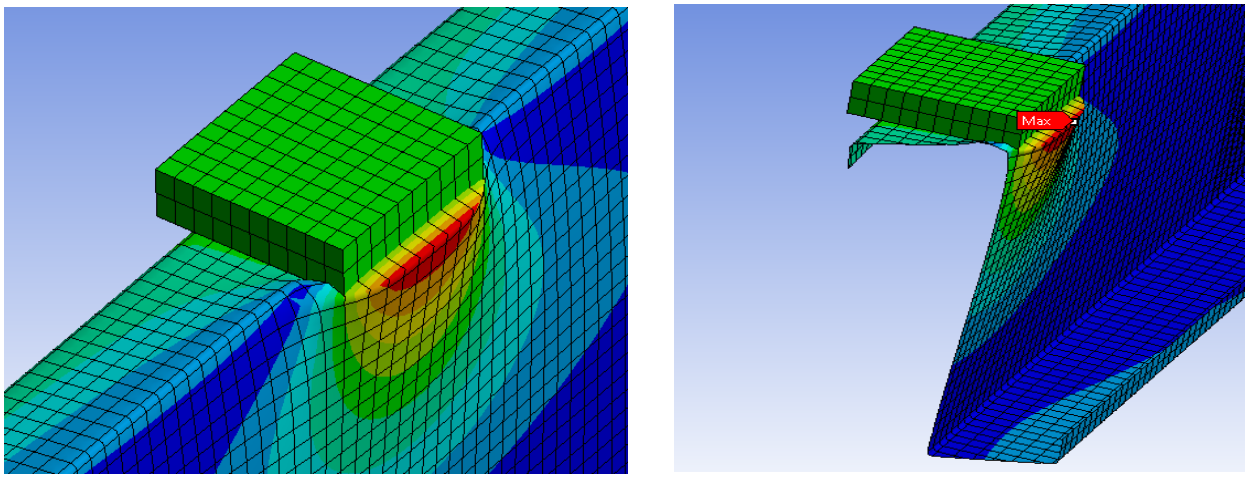


(a) Isometric view (b) Sectional view

Figure 68: Zed beam deformation analysis ( a ) top view & (b) sectional view

The deformation of the beam has clearly shown in the above picture (figure 68); the maximum amount of bending stress has seen in the middle of the section beam near the contact surface between the top-loading block and flange area of the beam.

The beam web starts bending in the middle section sand maximum bending stress is gradually distributed around the middle area of the web. similarly, the result of the bending stress in the bottom figures is recorded from individual simulation of FE - Beta (innovational model) and is shown in the blue graph of applied displacement vs. reaction force. The graph with different thickness range from 1mm, 1.5mm, 2mm, 3mm, and 4mm. It shows the change in reaction force for non-linear material after increasing thickness.

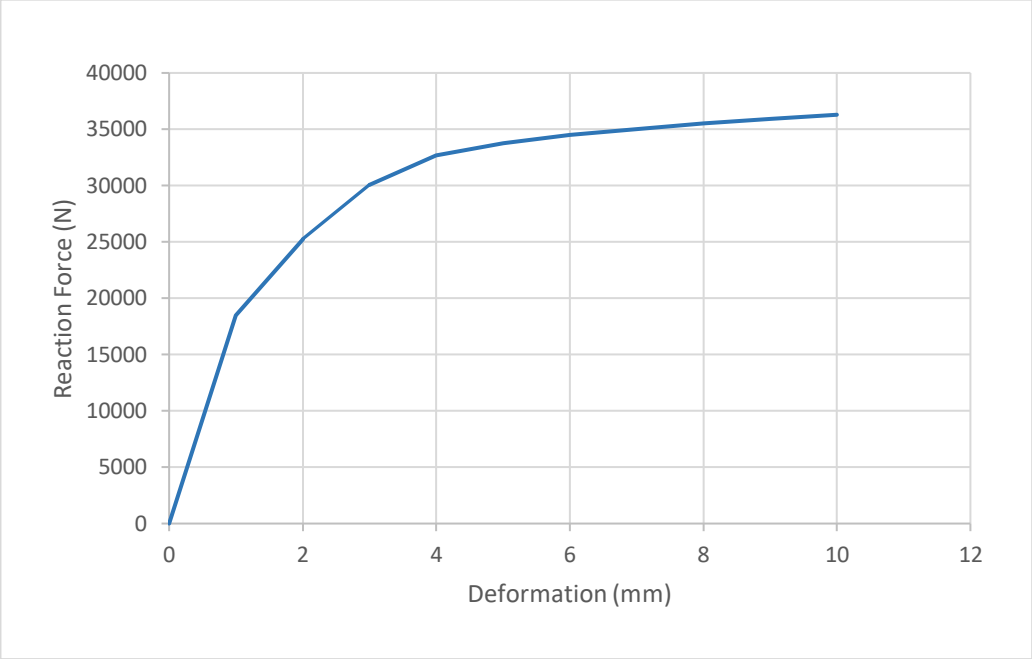


Figure 69: Beta model (zed) - Reaction force vs displacement (1mm thickness)

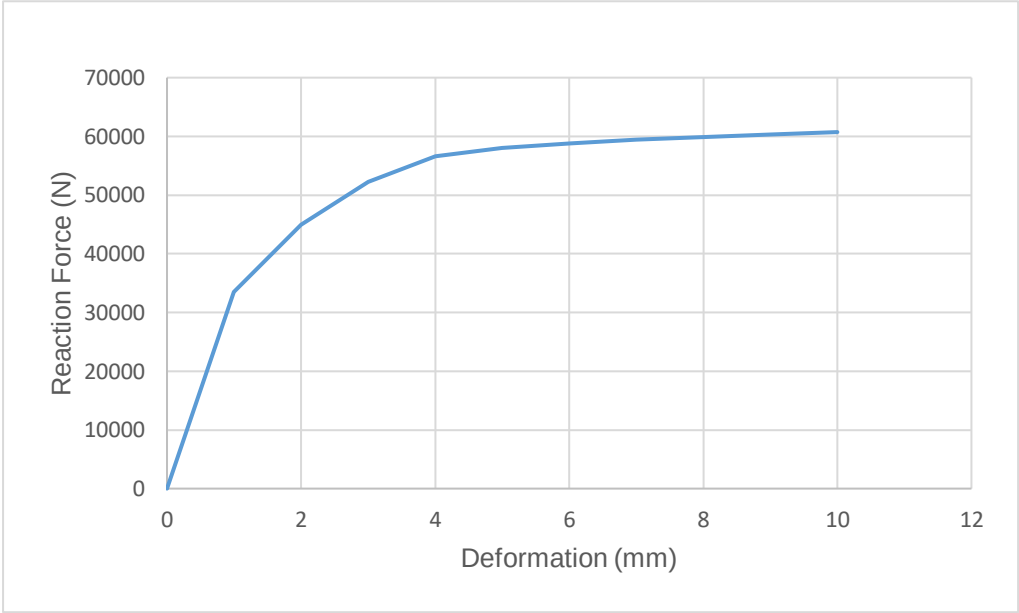


Figure 70: Beta model (zed) - Reaction force vs displacement (1.5mm thickness)

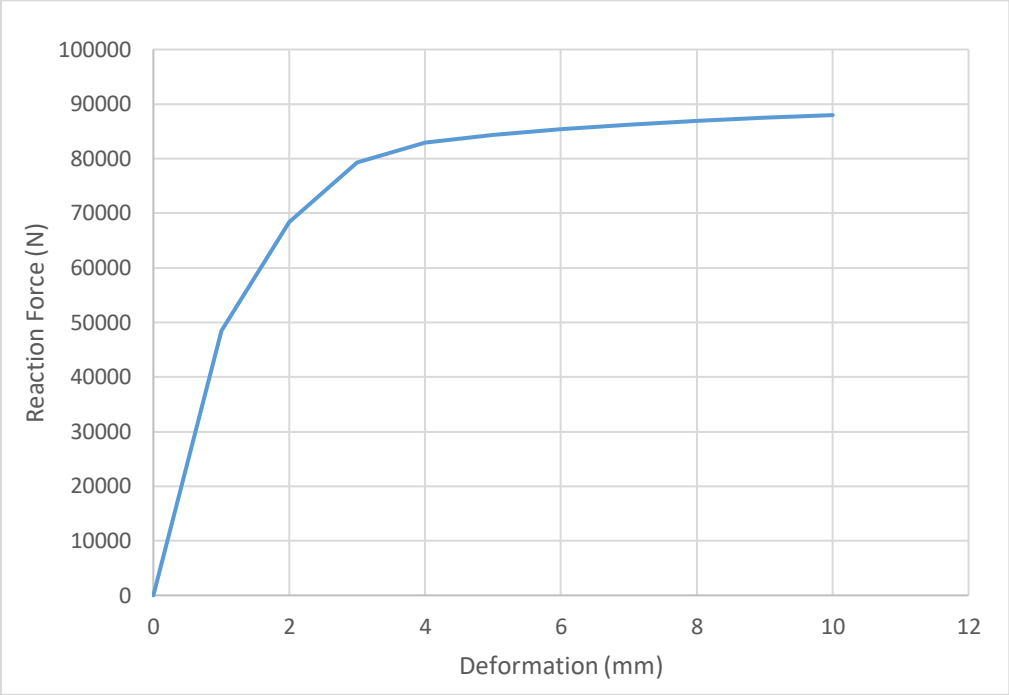


Figure 71: Beta model (zed) - Reaction force vs displacement (2mm thickness)

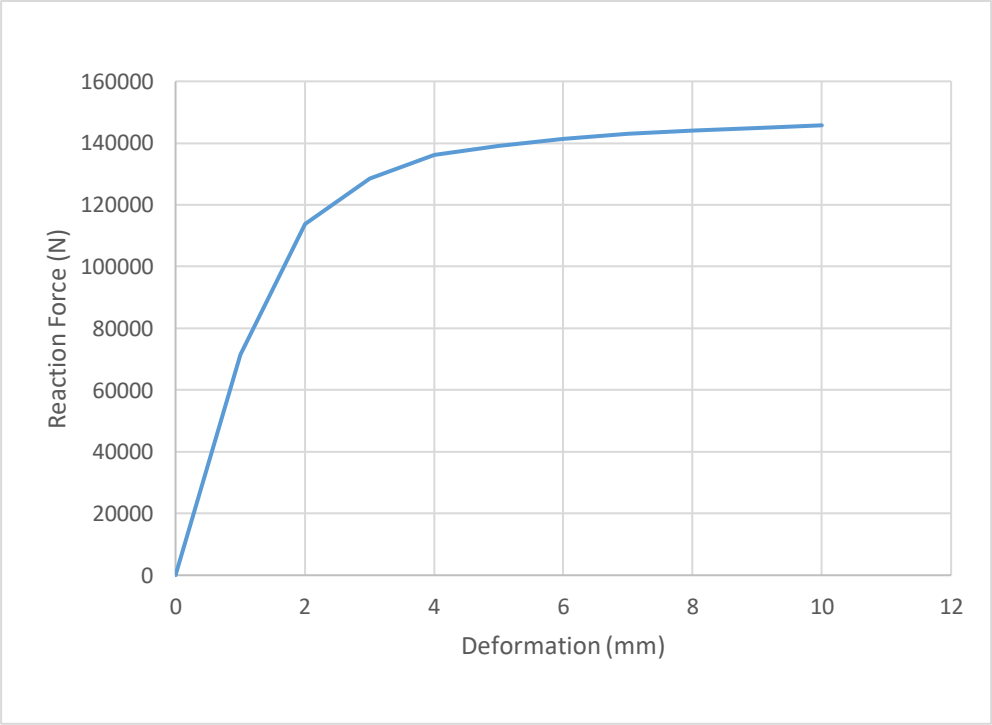


Figure 72: Beta model  (zed) - Reaction force vs displacement (3mm thickness)

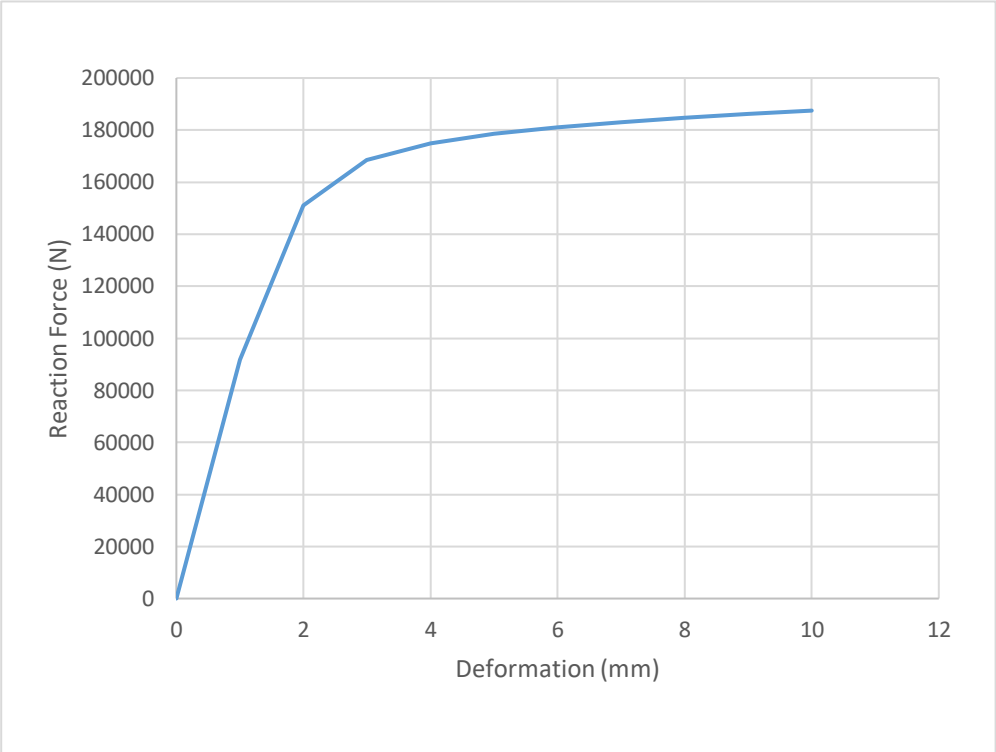


Figure 73: Beta model (zed) - Reaction force vs displacement (4mm thickness)

Table 6: Reaction force data of beta innovation model from different thickness

| Channel Section Thickness (mm) | Force Reaction (N) |
|---|---|
| 1 mm | 36288 N |
| 1.5 mm | 60724 N |
| 2 mm | 87983 N |
| 3 mm | 145750 N |
| 4 mm | 187480 N |

Similarly, individual simulation was performed again, in various thicknesses from 1mm to 4mm (shown in top table 6), to reproduce the testing conditions for validating the results, a parametric study was performed to measure the impact of undergoing different sections thickness.

According to the graph, the data obtained from individual 1mm to 4mm thickness simulation has shown increases in reaction force. overall no irregular or abrupt changes have been observed in maximum load between increasing variables, and they all obey the same linear trend (shown in figure 74).

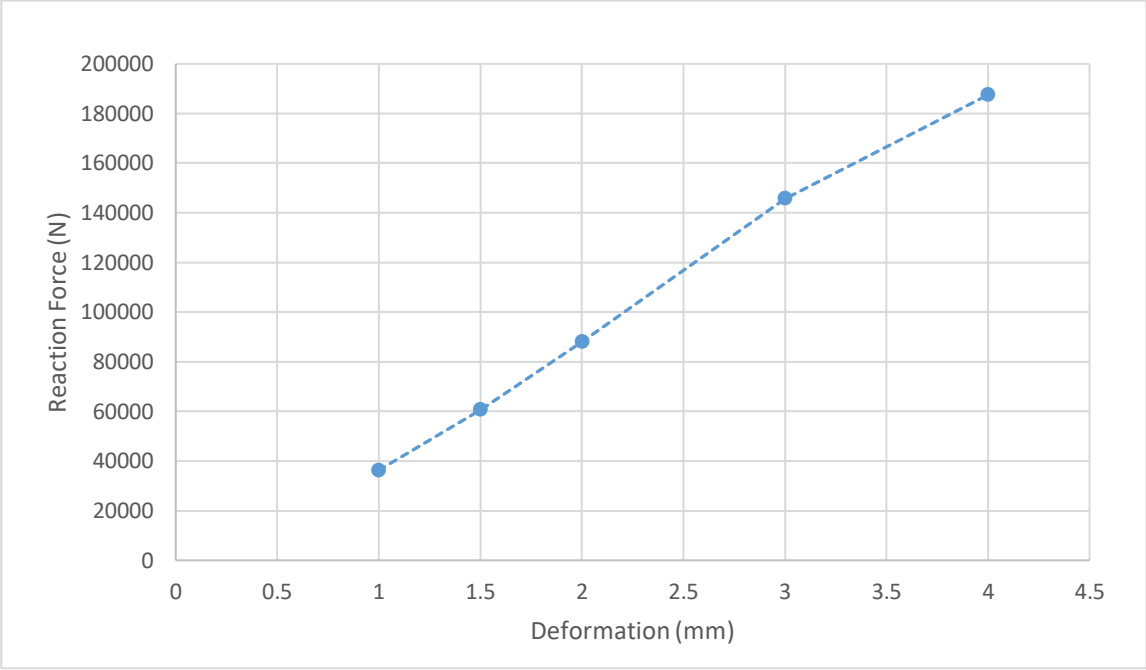


Figure 74: Beta - Zed model reaction force vs thickness

# 7.Conclusion & future works

This research aimed to create code that could parametrically model cold-shaped steel sections under various bending conditions. Section subject to simple three-point bending tests, as well as connection sections and contact behaviors, are all described by codes.

The correctness of the code was tested using parametric studies, which included changes in the thickness of the sections. All simulations result of FE surface body with various thicknesses can generate consistent results.

A comparison between the experimental data and FE simulation data is performed. This demonstrated that the code can correctly estimate the maximum reaction load that section could withstand, but there was a major stiffness error and it is considered to be caused due to connection inability to accurately reflect the strength of the bolt that holds the parts together.

It is therefore advised that extra work needs to be carried out to design a bolt-in FE model, the connection can be placed in between the holes to the surface, and a solid support model. the bolt's behavior can improve the FE simulation and the bolt should also contain weight for a more accurate result.

to achieve the more accurate result for innovation finite element alpha and beta model, the physical experiment needs to be carried out and comparison needs to be conducted between experimental result data and FE simulation result data.

## Appendix I (Data table from Lysaghte company)

**Standard range of LYSAGHT Zeds and Cees**

| Nominal section size (mm) | BMT (mm) |
|---|---|
| 100 | 1.0, 1.2, 1.5, 1.9 |
| 150 | 1.2, 1.5, 1.9, 2.4 |
| 200 | 1.5, 1.9, 2.4 |
| 250 | 1.9, 2.4 |
| 300 | 2.4, 3.0 |
| 350 | 3.0 |

## Appendix II (Lip channel data table from Tubecon company)

| | | | | | | | | | | |
|---|---|---|---|---|---|---|---|---|---|---|
| 200x100 x20x2,5 | 8,27 | 1,05 | 31,5 | 6,9 | 69 | 80,9 | 1,37 | 20 | 36 | 2,1 |
| 3 | 9,84 | 1,25 | 31,4 | 8,14 | 81,4 | 80,6 | 1,6 | 23,3 | 35,7 | 3,76 |
| 3,5 | 11,4 | 1,45 | 31,4 | 9,34 | 93,4 | 80,3 | 1,82 | 26,5 | 35,4 | 5,92 |
| 4,5 | 14,4 | 1,83 | 31,2 | 11,6 | 116 | 79,6 | 2,21 | 32,1 | 34,7 | 12,3 |
| | | | | | | | | | | |
| 225x75 x20x2,5 | 7,78 | 0,991 | 20,6 | 7,49 | 66,6 | 86,9 | 0,701 | 12,9 | 26,6 | 2,06 |
| 3 | 9,25 | 1,18 | 20,5 | 8,83 | 78,4 | 86,6 | 0,814 | 14,9 | 26,3 | 3,53 |
| 3,5 | 10,7 | 1,36 | 20,5 | 10,1 | 89,9 | 86,2 | 0,919 | 16,9 | 26 | 5,56 |
| 4,5 | 13,5 | 1,72 | 20,4 | 12,5 | 111 | 85,4 | 1,1 | 20,2 | 25,3 | 11,6 |
| | | | | | | | | | | |
| 225x100 x20x2,5 | 8,76 | 1,12 | 29,8 | 9,04 | 80,3 | 90 | 1,42 | 20,3 | 35,7 | 2,33 |
| 3 | 10,4 | 1,33 | 29,7 | 10,7 | 94,9 | 89,6 | 1,66 | 23,7 | 35,4 | 3,98 |
| 3,5 | 12,1 | 1,54 | 29,7 | 12,3 | 109 | 89,3 | 1,89 | 26,8 | 35,1 | 6,27 |
| 4,5 | 15,2 | 1,94 | 29,5 | 15,2 | 136 | 88,6 | 2,3 | 32,6 | 34,4 | 13,1 |
| | | | | | | | | | | |
| 250x65 x20x2,5 | 6,36 | 0,81 | 16,2 | 7,2 | 57,6 | 94,3 | 0,421 | 8,62 | 22,8 | 1,08 |
| 3 | 7,88 | 1 | 16,2 | 8,84 | 70,7 | 93,9 | 0,508 | 10,4 | 22,5 | 2,09 |
| 3,5 | 9,37 | 1,19 | 16,1 | 10,4 | 83,3 | 93,4 | 0,588 | 12 | 22,2 | 3,58 |
| | | | | | | | | | | |
| 250x75 x20x2,5 | 8,27 | 1,05 | 19,4 | 9,61 | 76,9 | 95,5 | 0,723 | 13 | 26,2 | 2,19 |
| 3 | 9,84 | 1,25 | 19,4 | 11,3 | 90,7 | 95,1 | 0,839 | 15,1 | 25,9 | 3,76 |
| 3,5 | 11,4 | 1,45 | 19,4 | 13 | 104 | 94,7 | 0,948 | 17 | 25,6 | 5,92 |
| 4,5 | 14,4 | 1,83 | 19,3 | 16,1 | 29 | 93,9 | 1,14 | 20,4 | 24,9 | 12,3 |

[Lip Channels (tubecon.co.za)]

## Appendix III (Lip and open channel data table from Tubecon company)

| Lip Channel Dimensions | | | Standard Material and Wall Thickness* | | |
|---|---|---|---|---|---|
| Width | Height | Lip | SAE1008 | S355 | Z275 (Pre-Galv) |
| 75 | 45 | 15 | 2mm-4mm | 2.5mm-4mm | 2mm |
| 75 | 50 | 20 | 2mm-4mm | 2.5mm-4mm | 2mm |
| 100 | 50 | 20 | 2mm-4mm | 2.5mm-4mm | 2mm |
| 125 | 50 | 20 | 2mm-4mm | 2.5mm-4mm | 2mm |
| 125 | 65 | 20 | 2mm-4mm | 2.5mm-4mm | 2mm |
| 125 | 75 | 20 | 2mm-4mm | 2.5mm-4mm | 2mm |
| 150 | 50 | 20 | 2mm-4mm | 2.5mm-4mm | 2mm |
| 150 | 75 | 20 | 2mm-4mm | 2.5mm-4mm | 2mm |
| 175 | 50 | 20 | 2mm-4mm | 2.5mm-4mm | 2mm |
| 175 | 75 | 20 | 2mm-4mm | 2.5mm-4mm | 2mm |
| 200 | 50 | 20 | 2mm-4mm | 2.5mm-4mm | 2mm |
| 200 | 75 | 20 | 2mm-4mm | 2.5mm-4mm | 2mm |
| 225 | 50 | 20 | 2mm-4mm | 2.5mm-4mm | 2mm |
| 225 | 75 | 20 | 2mm-4mm | 2.5mm-4mm | 2mm |
| 250 | 50 | 20 | 2mm-4mm | 2.5mm-4mm | 2mm |
| 250 | 75 | 20 | 2mm-4mm | 2.5mm-4mm | 2mm |
| 300 | 50 | 20 | 2mm-4mm | 2.5mm-4mm | 2mm |
| 300 | 75 | 20 | 2mm-4mm | 2.5mm-4mm | 2mm |
| 100 | 65 | 15 | 2mm-4mm | 2.5mm-4mm | 2mm |
| 150 | 65 | 20 | 2mm-4mm | 2.5mm-4mm | 2mm |
| 175 | 65 | 20 | 2mm-4mm | 2.5mm-4mm | 2mm |
| 200 | 65 | 20 | 2mm-4mm | 2.5mm-4mm | 2mm |
| 225 | 65 | 20 | 2mm-4mm | 2.5mm-4mm | 2mm |
| 250 | 65 | 20 | 2mm-4mm | 2.5mm-4mm | 2mm |
| 300 | 65 | 20 | 2mm-4mm | 2.5mm-4mm | 2mm |

[Lip & Open Channels | Tubecon]

## Appendix IV (Experimental data for channel1)

Table 7: Experimental channel section beam dimension

| **Channel Section Dimension** | |
|---|---|
| Web | 141.63mm |
| Flange | 52.90mm |
| Lip | 18.55mm |
| Thickness | 1.56mm |
| Fillet Radius | 2mm |
| Section span | 2400mm |

Table 8: Support block members dimension

| **Support Block Dimension** | |
|---|---|
| Length | 140mm |
| Width | 50mm |
| Height | 191.63mm (25mm above & below channel section) |

Table 9: Loading block member dimension

| **Loading block** | |
|---|---|
| Length | 120mm |
| Width | 50mm |
| Thickness | 25mm |

Table 10: Non-linear material properties

| **Non-linear Material properties** | |
|---|---|
| Young‘s modulus (E) | 203Gpa |
| Yield strength | 390Mpa |
| Poisson Ratio (V) | 0.3 |

# References


Park, Hong-Seok & Anh, Tran-Viet. (2011). Optimization of bending sequence in roll forming using neural network and genetic algorithm. Journal of Mechanical Science and Technology. 25. 2127-2136. 10.1007/s12206-011-0533-6.

Uzzaman, & Lim, James & Nash, David & Rhodes, Jim & Young, Ben. (2012). Parametric studies and design recommendations of cold-formed steel sections with web openings subjected to web crippling.

Uzzaman A, Lim J, Nash D, Rhodes J, Young B. Cold-formed steel sections with web openings subjected to web crippling under two-flange loading conditions—Part II: Parametric study and proposed design equations. Thin-Walled Structures. 2012; 56:79-87.

Mariam, M., Afendi, M. and Abdul Majid, M. (2017) Environmental Effect on Short-Beam Composite under Three-Point Bending Test. Key Engineering Materials. Vol.740, pp.17-24.

Senthilkumar, R., Sunil, T. and Jayabalan, P. (n.d.) Buckling Behaviour of Hollow Flange Channel Beam Sections in Bending.

(2021) [Online]. I-asem.org. Available: http://www.i-asem.org/publication_conf/asem17/2.SC/XH3B.2.SC1152_3828F1.pdf

(2021) [Online]. Pureadmin.qub.ac.uk. Available: https://pureadmin.qub.ac.uk/ws/files/124110817/Manuscript_Part_I.pdf

(2021) [Online]. I-asem.org. Available: http://www.i-asem.org/publication_conf/asem17/2.SC/XH3B.2.SC1152_3828F1.pdf

Bending Tests - an overview | ScienceDirect Topics. (2021) [Online]. Sciencedirect.com. Available: https://www.sciencedirect.com/topics/engineering/bending-tests

Steel connection – bolted connection - Surrey Steels - Steel fabricator and supplier in London. (2021) [Online]. Surrey Steels - Steel fabricator and supplier in London. Available: https://surreysteels.com/2019/02/25/steel-connection-bolted-connection

Lip & Open Channels | Tubecon. (2021) [Online]. Tubecon.co.za. Available: https://www.tubecon.co.za/en/products/lip-open-channels.html

Lipped Channel Galvanized & Uncoated - Steel and Pipes for Africa - Fencing | Tube | Automation of Gate Motors | Steel | Sheet | Roofing | Reinforcing | Handrailings | Palisade Fencing | Bolts & Nuts | Locks | Galvanised Steel | Welding Consumables | Paint | Power Tools | Hardware. (2021) [Online]. Steel and Pipes for Africa - Fencing | Tube | Automation of Gate Motors | Steel | Sheet | Roofing | Reinforcing | Handrailings | Palisade Fencing | Bolts & Nuts | Locks | Galvanised Steel | Welding Consumables | Paint | Power Tools | Hardware. Available: http://steelandpipes.co.za/mild-steel-2/lipped-channel-galvanized-uncoated-mild-steel

(2021) [Online]. Consteel.com.sg. Available: http://www.consteel.com.sg/downloadfiles/consteel2006.pdf

(2021) [Online]. Legrand.co.uk. Available: https://www.legrand.co.uk/media/4377/beama_tray_and_ladder_best_practice_guide.pdf

(2021) [Online]. Professionals.lysaght.com. Available: https://professionals.lysaght.com/sites/default/files/LysaghtZedCeesPart1July2014.pdf

(2021) [Online]. Orbi.uliege.be. Available: https://orbi.uliege.be/bitstream/2268/143198/1/FullPaper_JOUAN.pdf

(2021) [Online]. Drahmednagib.com. Available: https://drahmednagib.com/CAD_2018/Lecture_3_Meshing_2.pdf

(2021) [Online]. Egr.msu.edu. Available: https://www.egr.msu.edu/~harichan/classes/ce405/chap2.pdf

(2021) [Online]. Ce.memphis.edu. Available: http://www.ce.memphis.edu/4135/PDF/Notes/Chapt_5_3.pdf

(2021) [Online]. Kdm.p.lodz.pl. Available: http://www.kdm.p.lodz.pl/articles/2013/17_2_2M_K.pdf